5-2020

A Historical Account of Atmospheric Lead Deposition in Basin Pond, Fayette, Maine

Samuel Kent Onion
sonion@bates.edu

Recommended Citation

Onion, Samuel Kent, "A Historical Account of Atmospheric Lead Deposition in Basin Pond, Fayette, Maine" (2020). *Standard Theses*. 47.
https://scarab.bates.edu/geology_theses/47

A Historical Account of Atmospheric Lead Deposition in Basin Pond, Fayette, Maine

A Senior Thesis
Presented to
The Faculty of the Department of Geology
Bates College

In partial fulfillment of the requirements for the
Degree of Bachelor of Arts

By

Samuel Kent Onion
Lewiston, Maine
December 13, 2019

Acknowledgements

I would like to thank my thesis advisor Professor Beverly Johnson for her constant support, work, and patience that went into this project and revising it to what it is today. Thank you to Phil Dostie for his unending positivity and enthusiasm, and helping me daily for several months with the lab work involved in this project. Also thank you to Professor Mike Retelle for his support and input in looking at Basin Pond sediments. Thank you to Pete Schlax for helping me find sources and correlations that aligned with my data and background research that went into the project. Thank you to the geology class of 2020 and all other professors in the geology department for their support and feedback throughout the project. Thank you to the Bates Student Research Fund which funded the creation of thin sections for my thesis. Thank you to the company Arizona Thin Sections for their work in creating the thin sections for my thesis. Finally, I would like to thank my family for their support and kindness throughout the project. This work would not have been possible without any of you, so thank you all.

Table of Contents

Table of Figures

Abstract

Global anthropogenic activity and resultant environmental emissions significantly alter atmospheric lead concentration. Records of atmospheric lead emissions are preserved throughout the world in lake sediments. Basin Pond, in Fayette, Maine, at 32 meters deep and .109 km^2 in surface area, is devoid of any nearby anthropogenic impacts, and therefore records the variance in atmospheric anthropogenic pollutants alone in its undisturbed varved sediment. A freeze core was collected from Basin Pond to analyze the historic atmospheric lead deposition throughout the entire core. Thin sections of the core were created in attempts to find an age model for the core and the lead concentration was analyzed throughout the core using ICP-OES analysis. The sediments in the thin sections were muddled, so an average of age models from Miller, (2015) was used to estimate the relative age of sedimentation throughout the core. Results indicated 3 major trends in atmospheric lead concentration throughout the core, with low initial background levels at ~5 mg Pb/kg sediment and peak levels at ~120 mg Pb/kg sediment. A rise and fall from 1590 to 1681 may indicate increased mining in Virginia at the time followed by the rise of tobacco plantations. A rise and fall from 1895 – 1987 may indicate the increased usage of leaded gasoline followed by the phasing out of lead as a gasoline additive in the 1970s. A rise from the 1990s to the present could indicate recent increased lead mining and fossil fuel emissions from China and a few other countries. This final rise in lead concentration goes against the observed results for lakes throughout the United States, and should be investigated further to confirm its validity.

Chapter 1: Introduction

1.1. Purpose

Lead exists naturally within the earth, and is dispersed through several natural and anthropogenic processes. The rise of humanity brought upon long-distance dispersal of lead, raising the lead levels in the environment through anthropogenic activity and industrialization. The varying changes in lead concentrations can be tracked in great detail using varved sequences within anoxic lakes, which carefully record, in yearly increments, exact details of environmental change over time. Basin Pond in Fayette, Maine, is one such lake, and contains hundreds of years of environmental data stored in its varved sequence. This study examines the changing environment and atmospheric conditions around Basin Pond, in Fayette, Maine through the tracking of lead concentrations using induced coupled plasma, optical emissions spectrometry (ICP-OES) analysis and thin sectional sedimentary analysis of varves within the sediment.

1.2. Study Site Geology

During the Acadian Orogeny in the early Devonian time period, several granitic plutons formed in the crust as a result of subduction of the Avalon plate under Gander (Bradley et al., 1999). Intrusion of these Devonian plutons formed contact aureoles in the surrounding country rock (Guidotti, 1989). The Neoacadian orogeny, occurring after the emplacement of the Acadian plutons, allowed for delamination of the crust, which thinned the crust significantly, and greatly increased the temperature of the crust, resulting in high temperature low pressure metamorphosis of modern-day southern Maine (figure 1.1; Murphy et al., 2007). In the Carboniferous period after the Acadian Orogeny, a late heating event from the Acadian orogeny produced the Sebago Granite pluton, slightly metamorphosing the surrounding rock in the southern third of Maine (Guidotti, 1989). Through erosion of the rock, over hundreds of millions of years, the plutons rose to the surface of the earth. Basin Pond exists on top of one of these major plutons in the Livermore quadrangle, and it is composed of quartz, plagioclase, microcline, muscovite, biotite, and chlorite (figure 1.2; Frost, 2005).

25,000 years ago, the Laurentide ice sheet covered the entirety of Maine (Thompson and Smith, 2008). Approximately 14,000 years ago, glacial melting started to erode the underlying rocks, with the melting front reaching the current location of Basin Pond 13,200 years ago (figure 1.3; Borns et al., 2004). The Laurentide ice sheet retreated to the northwest, resulting in the deposition of glacial sediments and creation of lakes (Borns et al., 2004). The area immediately around Basin pond is covered in a thin layer (<10 ft thick) of till with silt to gravel-sized sediment; eskers and glaciomarine sediments exist to the west of the pond in the same quadrant (figure 1.4; Thompson and Smith, 2008).

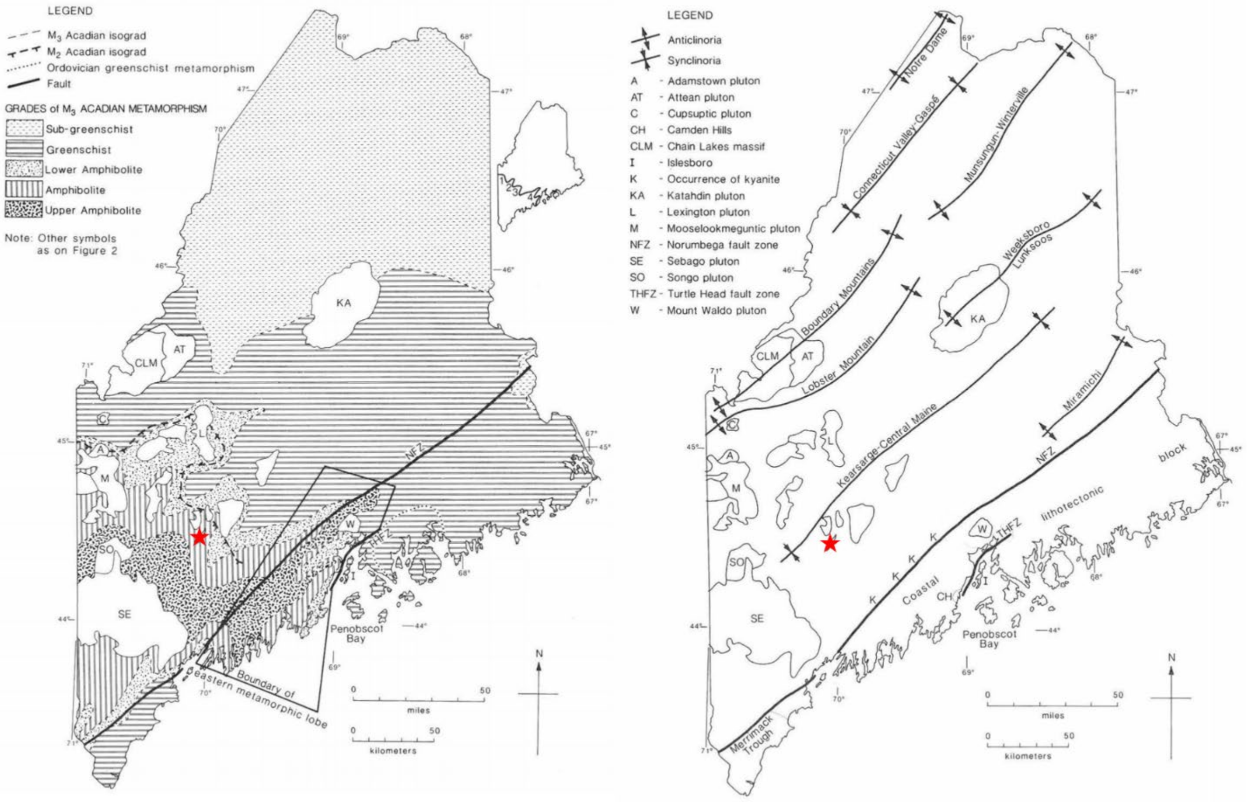

Figure 1.1. Metamorphic grades of rock within the state (left) with higher grades generally in the southwestern corner of Maine, and several plutons emplaced in the Devonian (right) (From Guidotti, 1989). The red stars mark the locality of Basin Pond.

Figure 1.2. Bedrock map of the region around Basin Pond, labeled with a red star. The blue D1 formations are plutons emplaced in the Devonian time period, the yellow Ss formation is the Sillurian Sangerville Formation, and the green Ssl formation is the Sillurian Sangerville limestone member (From Osberg et al., 1985).

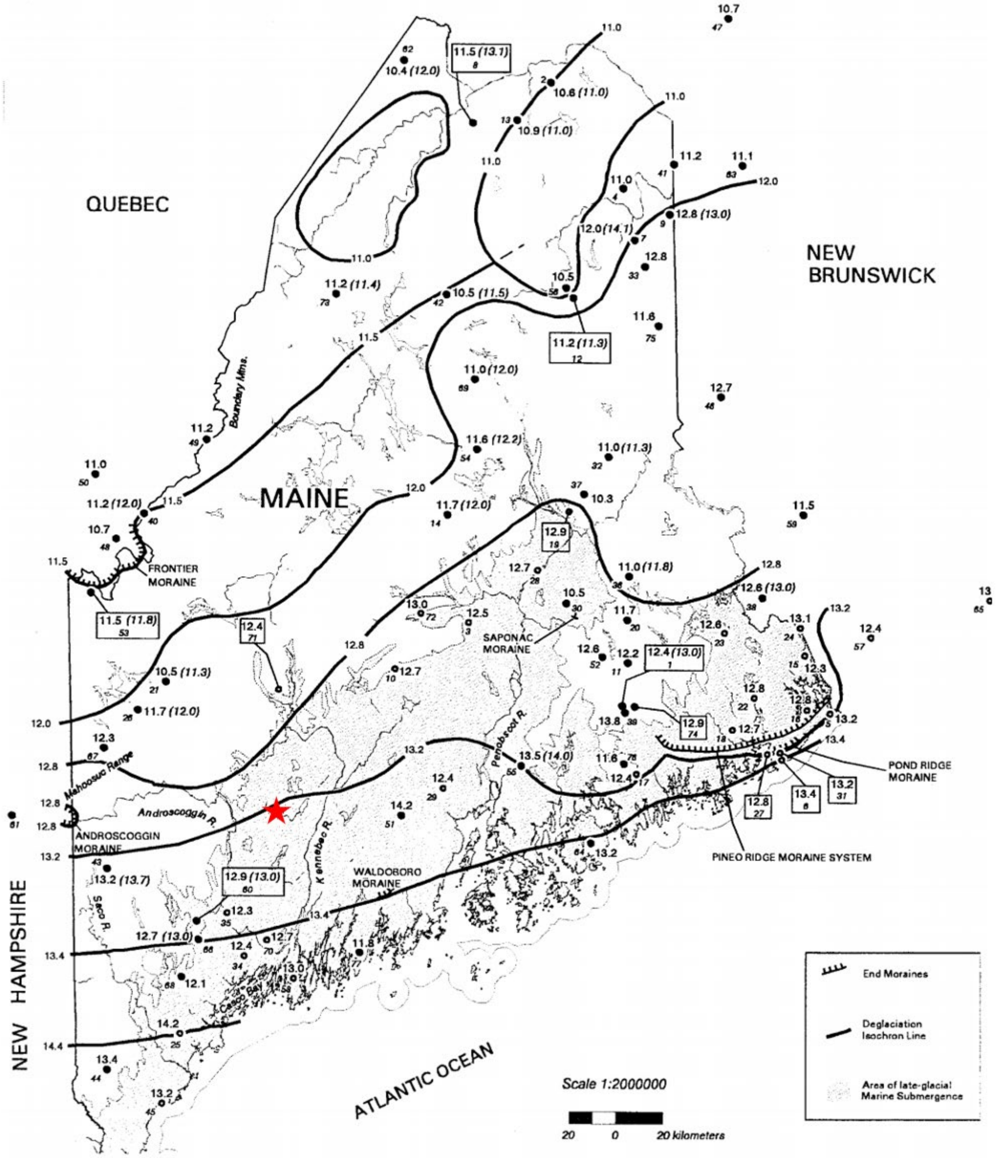

Figure 1.3. Map of Maine showing times of glacial retreat (From Borns et al., 2004).

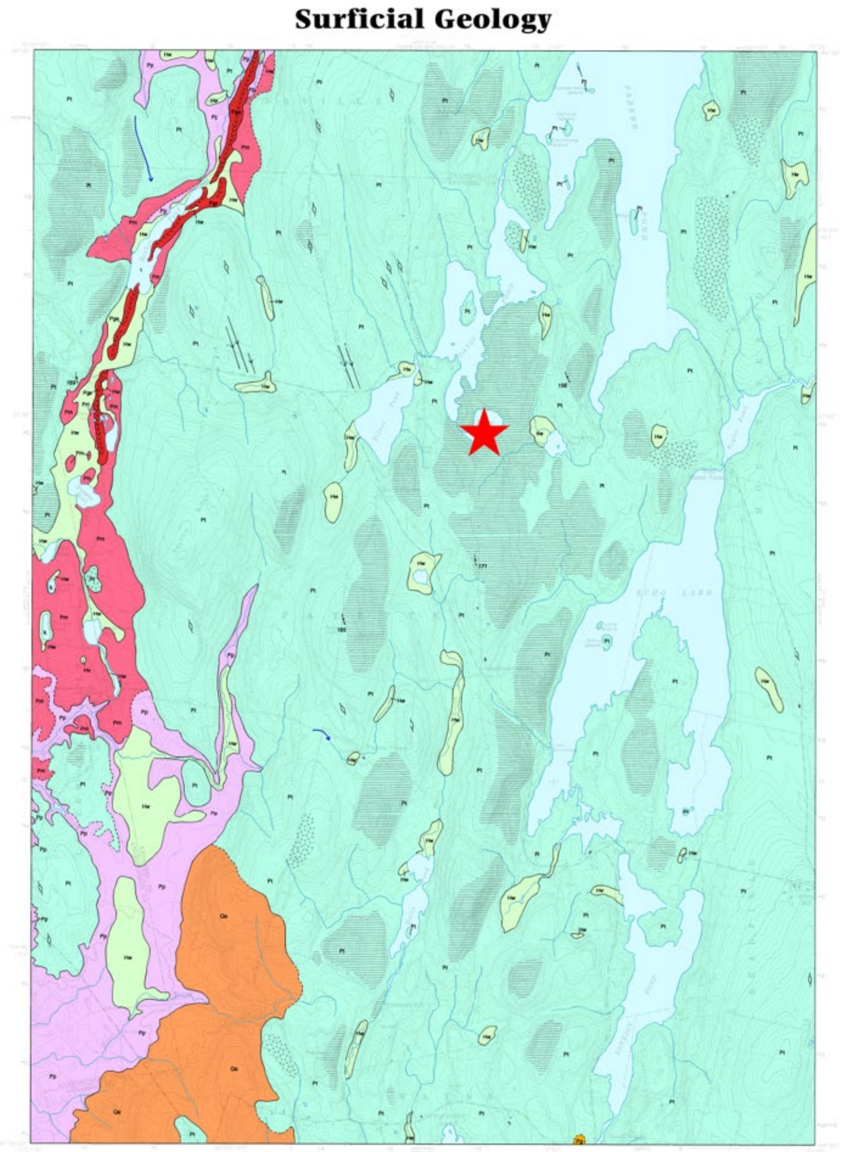

Figure 1.4. Surficial geology map of the study site, and Basin Pond labelled with the red star where the dark green layers are glacial till deposits, the light green layers are wetland deposits, the orange layers are Eolian deposits, the red layers are esker deposits, the lighter red layers are glaciomarine sediments, and the light purple layers are the Presumpscot Formation (From Thompson and Smith, 2008).

Basin Pond, at 32 meters deep and .109 km^2 in surface area, is an anomalous lake within central Maine due to its unique geometry (U.S. Geological Survey, 1996). Its small surface area and great depth allows for a lack of mixing to occur in the lake and low oxygen levels in the lower water column resulting in the accumulation of a varved sediment structure (Zolitschka, 2007). Lacustrine varves are natural sedimentary layers which show the undisturbed history of sedimentation (Zolitschka, 2007). They are often found in deep lakes with small surface areas and low oxygen contents that ice over in the winter to allow for the alteration between diatom blooms in the warmer months and organic and minerogenic detritus in the winter, showing up as the alteration between light and dark layers (Zolitschka, 2007). The sediments in Basin Pond are rich in organics, and originate directly from the surrounding catchment area (Miller, 2015). Sedimentation at Basin Pond occurs from runoff in the local watershed and regional atmospheric deposition.

Basin Pond is situated in an undeveloped area of Fayette, Maine, at 44° 27’N, 70° 03’W (figure 1.5), with steep banks to the south, northeast, and west, and shallow inclines elsewhere (U.S. Geological Survey, 1996). The lake has one outlet on the southwestern side and no inlets, which helps to preserve its pristine condition (figure 1.6; U.S. Geological Survey, 1996). The pond is a perfect study site to test for regional atmospheric lead deposition over the years because of its relative isolation from human activity, natural lead sources, and undisturbed sediment.

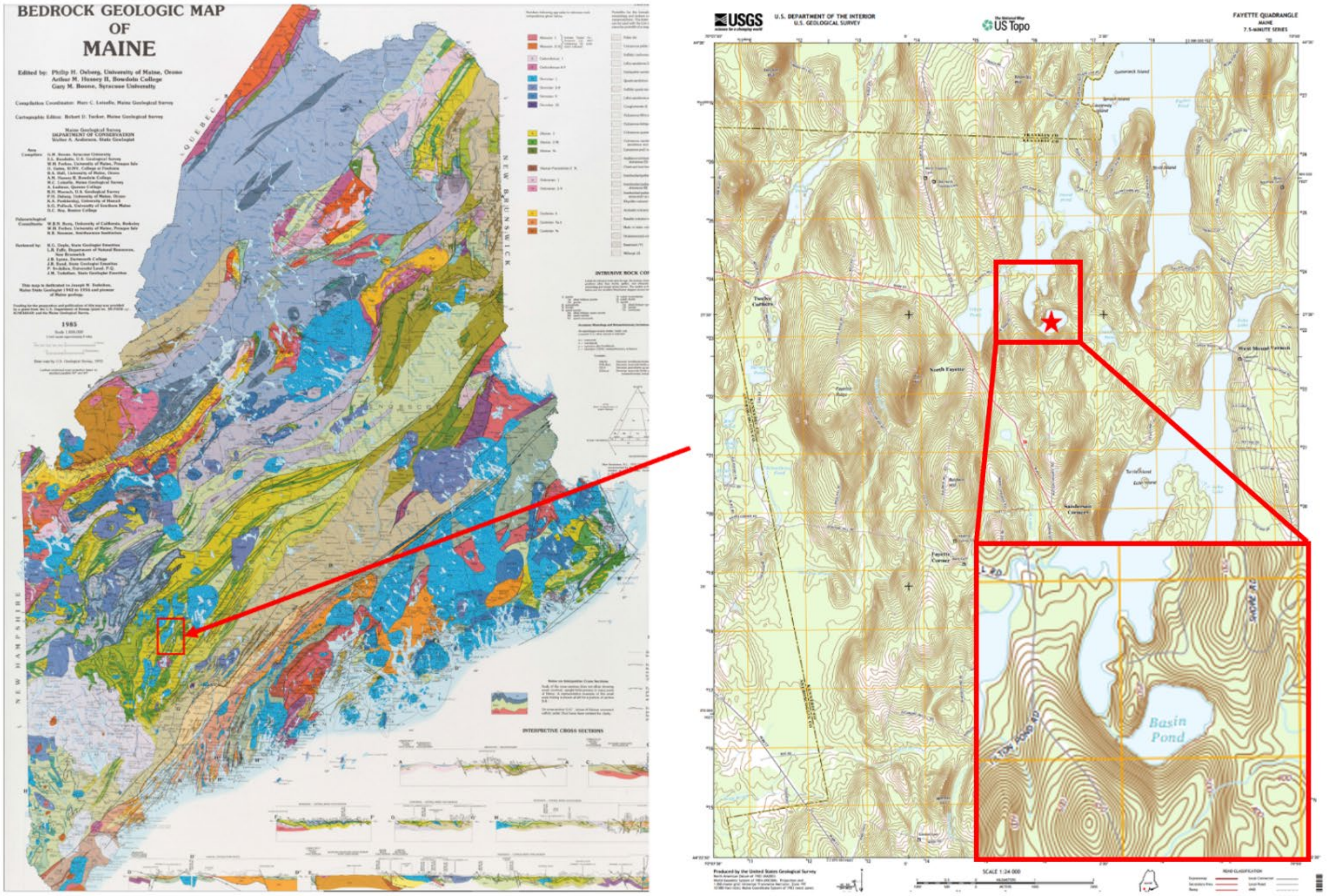

Figure 1.5. The right image depicts the location of Basin Pond on a topographical map of the region with a close up of the study site (modified from U.S. Geological Survey, 1996). The left image shows the location of the quadrant within the Bedrock Geologic Map of Maine (From Osberg et al., 1985).

Figure 1.6. Aerial photo of Basin Pond with the location of the outlet shown with the red arrow.

1.3. Background Information

Lead is a versatile metal and has several uses in industry. Due to its chemical resistance, it is commonly used to line pipes containing corrosive substances (Holland and Turekian, 2004). It is also used to create storage batteries and radiation shields (Holland and Turekian, 2004). To improve the efficiency of car engines, lead was used as an additive to gasoline, but because of the resulting pollution to the environment, this usage was outlawed (Holland and Turekian, 2004).

Lead is emitted into the environment through several natural and anthropogenic pathways. Erosion or dissolution of lead-concentrated rocks and volcanic activity naturally release lead particulates, and fossil fuel combustion, mining or smelting of lead, and waste incineration all contribute to anthropogenic lead emissions (Holland and Turekian, 2004). As an aerosol, lead travels through the atmosphere before fallout through dry or wet deposition over terrestrial or aquatic systems (Settle and Patterson, 1982). As an ion dissolved in water, lead travels through groundwater and fluvial systems, leading to lead deposition in the soils, and ocean or lake basins (Holland and Turekian, 2004).

Lacustrine sediments form through several different processes. Mineral particles from fluvial and atmospheric inputs form clastic sediments which settle to the bottom of the lake, biological productivity in the lake results in the creation of organic sediment layers, and chemical precipitation of minerals in the water column results in evaporitic sedimentation (figure 1.7; Zolitschka and Enters, 2009). Atmospheric lead, once introduced to the water column, initially exists as a free-floating ion, and then eventually either precipitates out of the water into the sediment, or sinks down to the bottom of the lake, binding with the sediment (Holland and Turekian, 2004).

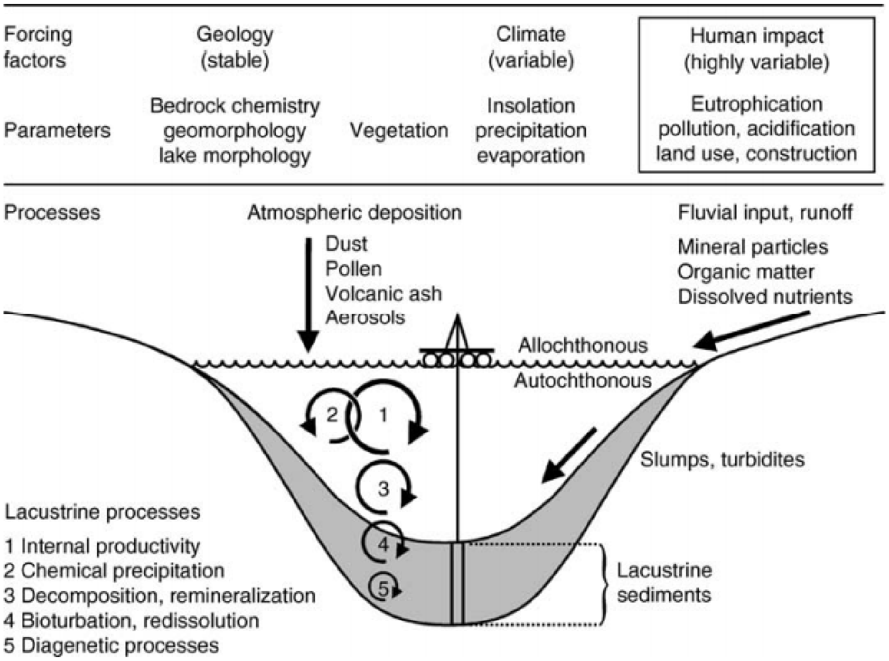

Figure 1.7. Processes leading to sedimentation in lakes, with chemical precipitation and remineralization driving the overall deposition of atmospheric lead in sediment (From Zolitschka and Enters, 2009)

Lead is a toxic substance to the environment and humanity, and is present in the soils, waters, and atmosphere of earth (Tiwari et al., 2013). Due to its prominence in the environment, it is easily contracted by human beings through ingestion of contaminated plants, inhalation of contaminated atmosphere, and drinking of contaminated water (Tiwari et al., 2013). Once in the body, it is difficult to remove and can result in impairment of the cognitive development of children, or in large concentrations, death (Tiwari et al., 2013).

Graney et al., (1995), describes the concentrations of 4 lead isotopes and their isotopic ratios within different sediment samples in the great lakes (figure 1.8). Higher isotopic ratios of Pb207/Pb206 and lower Pb208/Pb204 ratios indicate more thorogenic anthropogenic inputs coming from coal and ore smelting, whereas lower Pb207/Pb206 and higher Pb208/Pb204 ratios indicate more uranogenic anthropogenic inputs, specifically from the usage of leaded gasoline (figure 1.8; Graney et al., 1995). More coal burning and ore smelting occurred from 1860-1900 and more leaded gasoline burning occurred from the 1920s to the 1970s, falling from the 1970s to the present (figure 1.9; Graney et al., 1995).

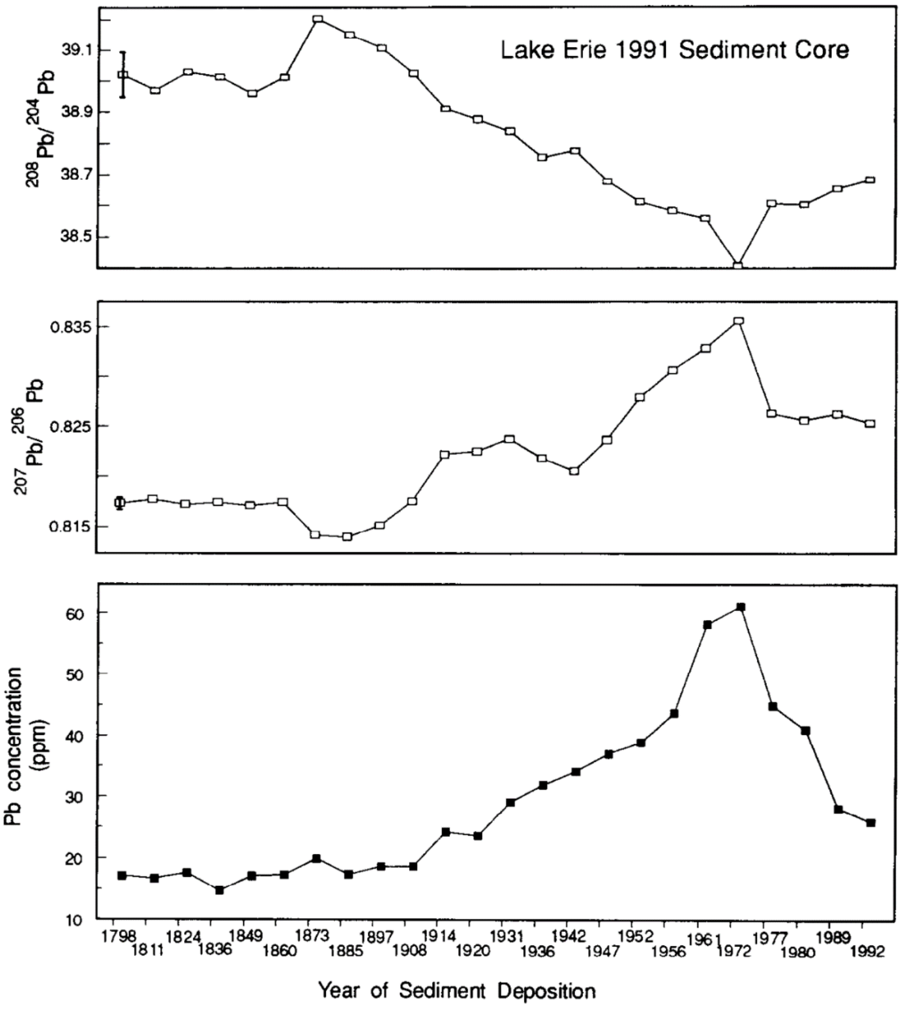

Figure 1.8. Lead concentration as a function of time with isotopic ratios showing higher proportions of various isotopes at different times (From Graney et al., 1995).

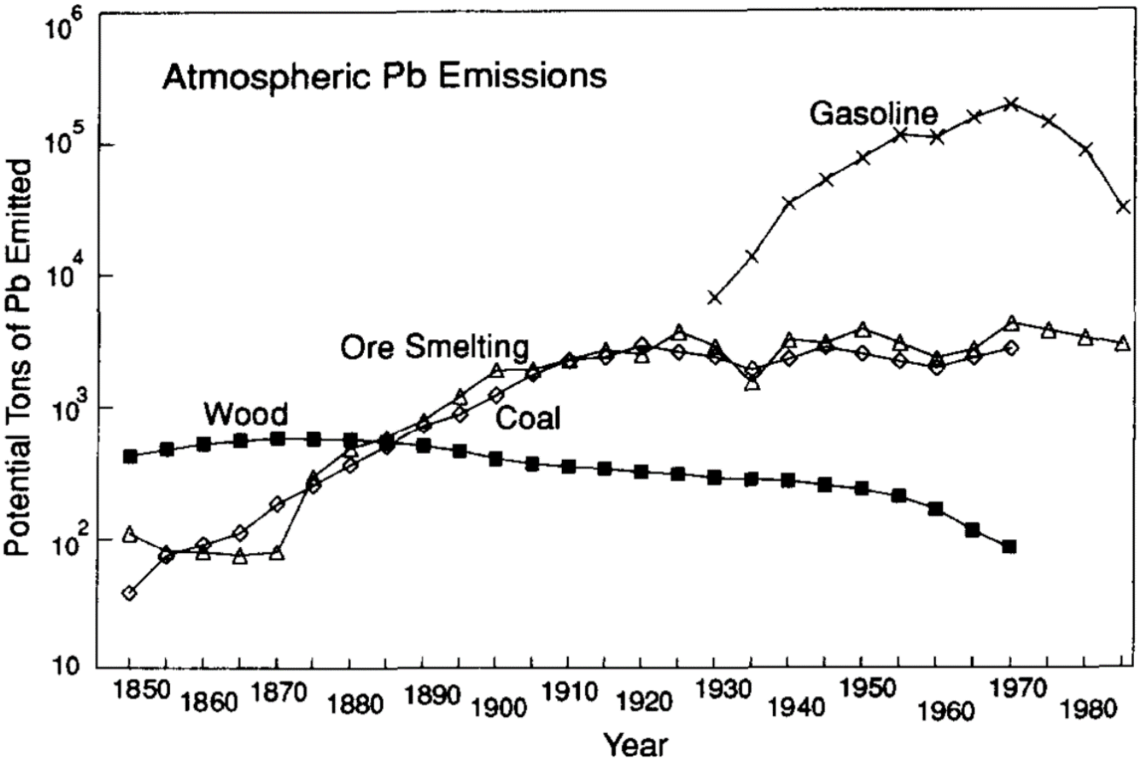

Figure 1.9. The various sources of atmospheric lead contaminants from 1850 to 1980 in the United States determined using estimation of emissions (From Graney et al., 1995).

Studies completed in the United States provide similar trends (with minor variations) in respect to past atmospheric lead deposition. In studies completed by Graney et al., (1995), Siver and Wozniak, (2001), Norton et al. (1995), and Callender and Metre, (1997), studying lakes in the mid-eastern United States, there is an overall trend in lead concentration and accumulation rates from the 1920s to the 1970s which shows the effects of the Clean Air Act, passed in the 1970s, banning the usage of leaded gasoline (figure 1.10). Additionally, Holland and Turekian, (2004) found that throughout the United States, there was an overall decreasing trend in lead concentration within lake sediment from 1975 for studies that they compiled (figure 1.11). Though the bioturbation of these lakes likely limits the certainty associated with each age model calculated, these trends were anticipated in Basin Pond as well.

Figure 1.10. The locations of various studies done throughout the US with respect to Basin Pond.

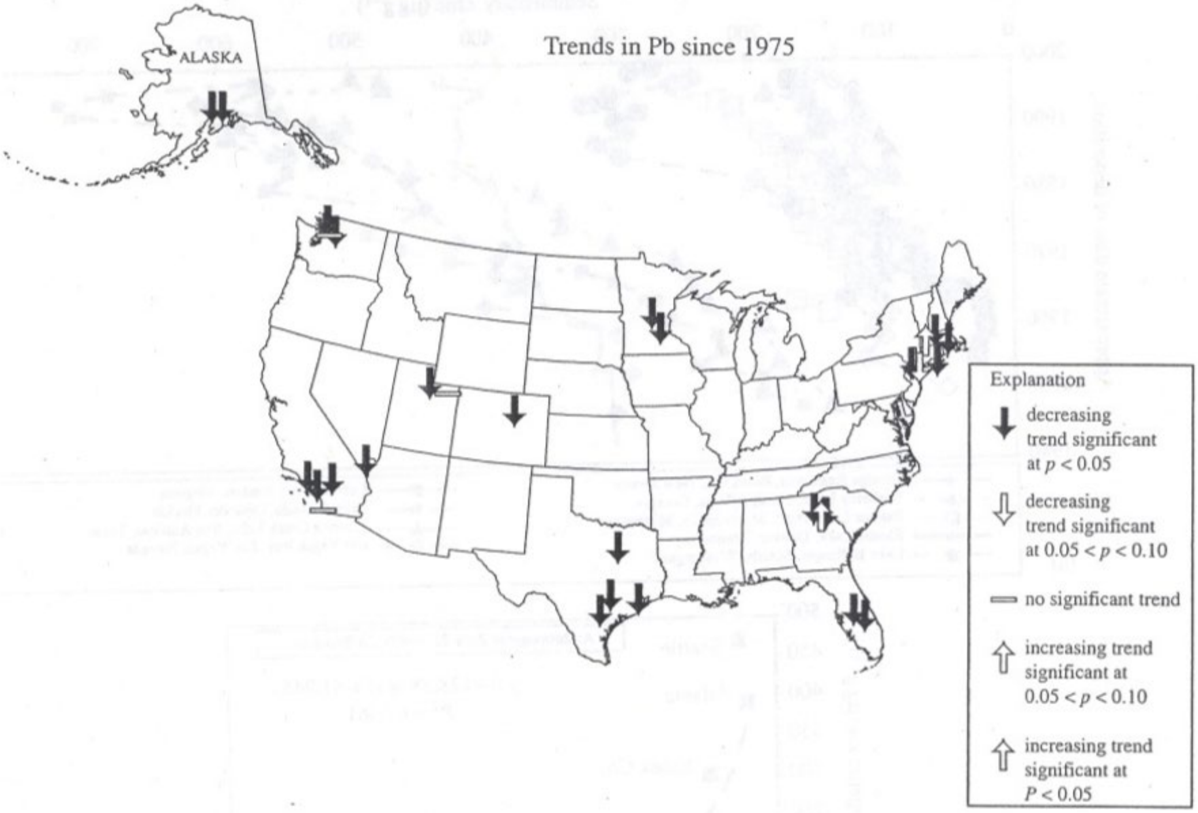

Figure 1.11. The overall decreasing trend in lead concentration throughout the United States (From Holland and Turekian, 2004).

1.4. Transport Mechanisms

1.4.1. National and International Winds

North American winds generally travel from west to east, transporting aerosols from southeastern Canada, and the southwestern United States to Maine (Eberle, 2008). Prevailing wind directions then suggest that sources of national and international atmospheric lead pollution affecting Basin Pond would come from these localities (figure 1.12). Global wind patterns show that the northern hemisphere exhibits winds travelling from west to east and major pollutant pathways follow the general flow in this region (figure 1.13; Marx and McGowan, 2010).

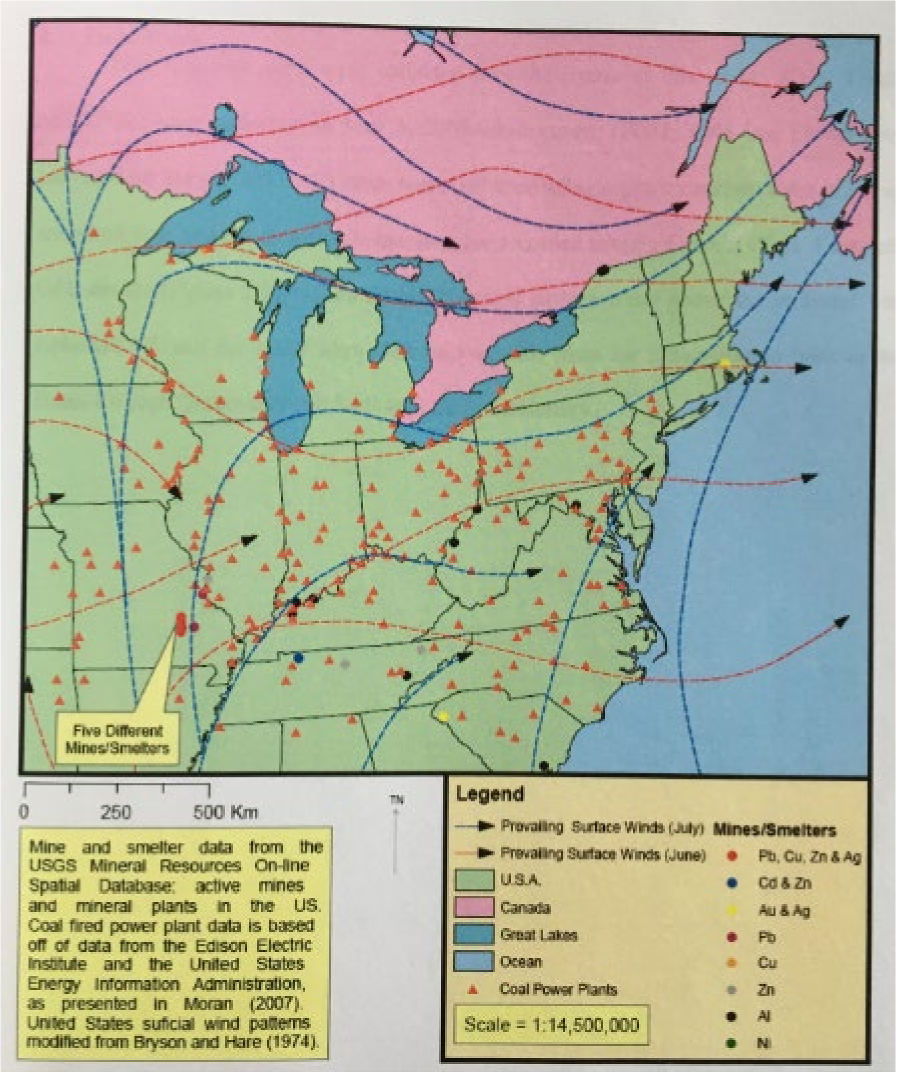

Mine and smelter data from the USGS Mineral Resources On-line Spatial Database: active mines and mineral plants in the US. Coal fired power plant data is based off of data from the Edison Electric Institute and the United States Energy Information Administration, as presented in Moran (2007). United States suficial wind patterns modified from Bryson and Hare (1974).

Figure 1.12. Wind currents throughout the eastern United States with mines and power plant locations in the United States (From Eberle, 2008). The blue lines show wind directions in July and red lines show wind directions in June.

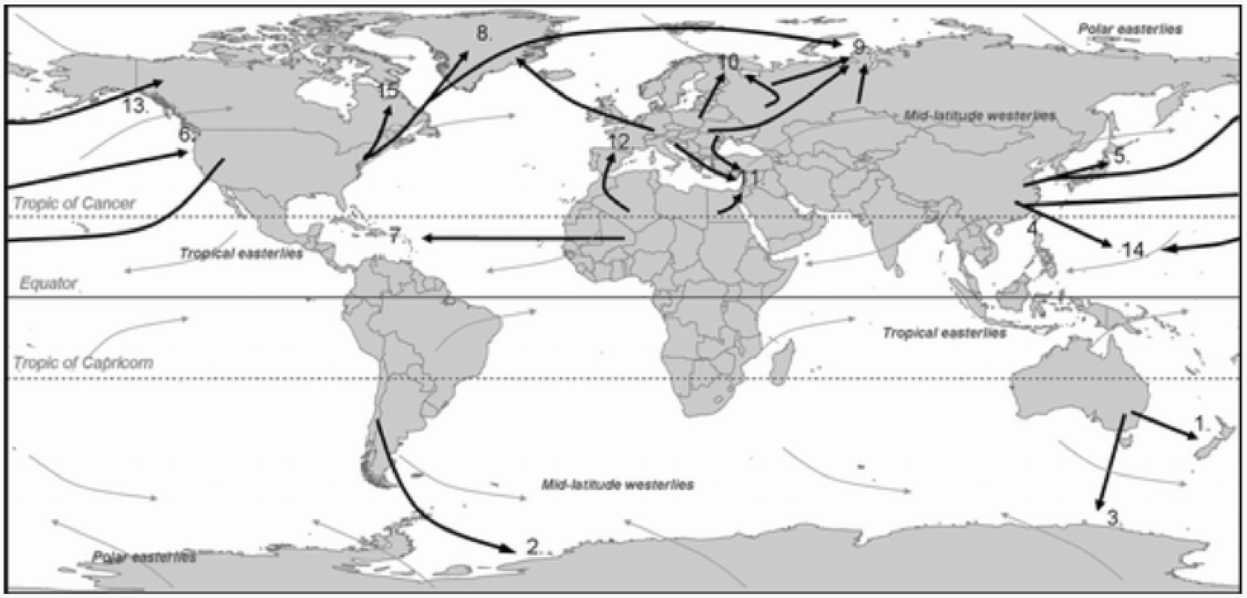

Figure 1.13. Wind currents and pollutant pathways around the world (From Marx and McGowan, 2010).

1.4.2. Seasonal and Annual Winds and Precipitation in Fayette, Maine

According to "Average weather in Fayette, Maine, United States" (https://weatherspark.com) in Fayette, Maine, winds generally come from the western direction with northwestern winds dominating in the winter and southwestern winds dominating in the summer (figure 1.14). Greater precipitation occurs during the summer months whereas lower overall precipitation occurs in the winter (https://weatherspark.com; figure 1.15). These data suggest that greater wet deposition occurs in the summer months than the winter months with winds coming from the southwest. Historically, Basin Pond varves indicate great variability in precipitation rates, with a general increase in precipitation over time from the late 1800's to today (Miller, 2015).

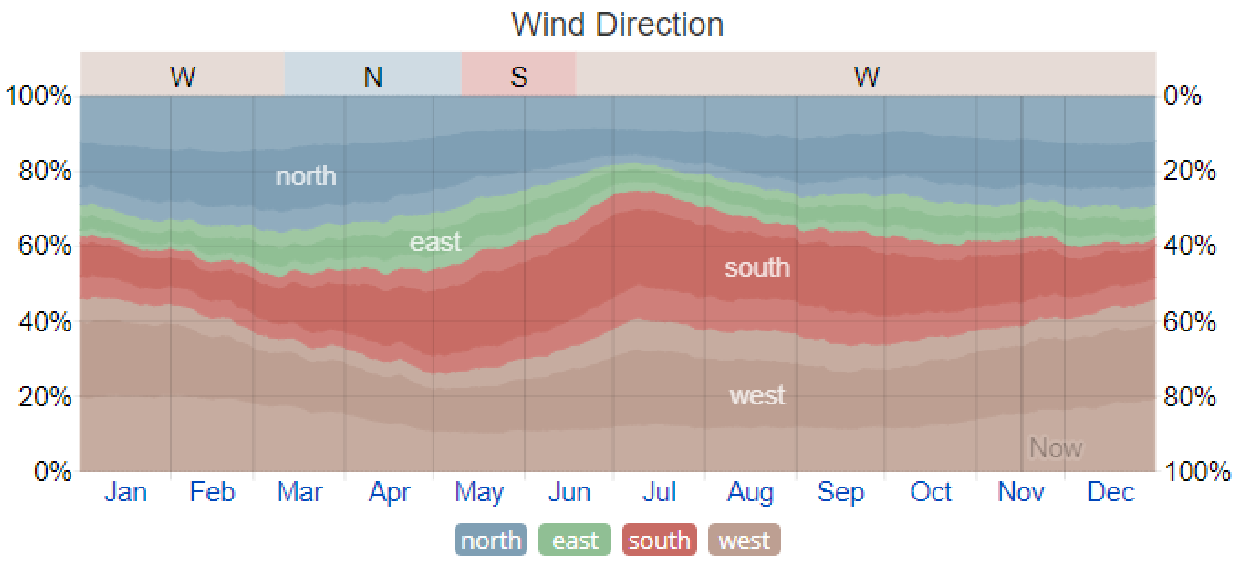

Figure 1.14. Seasonal wind directions in Fayette, Maine (https://weatherspark.com).

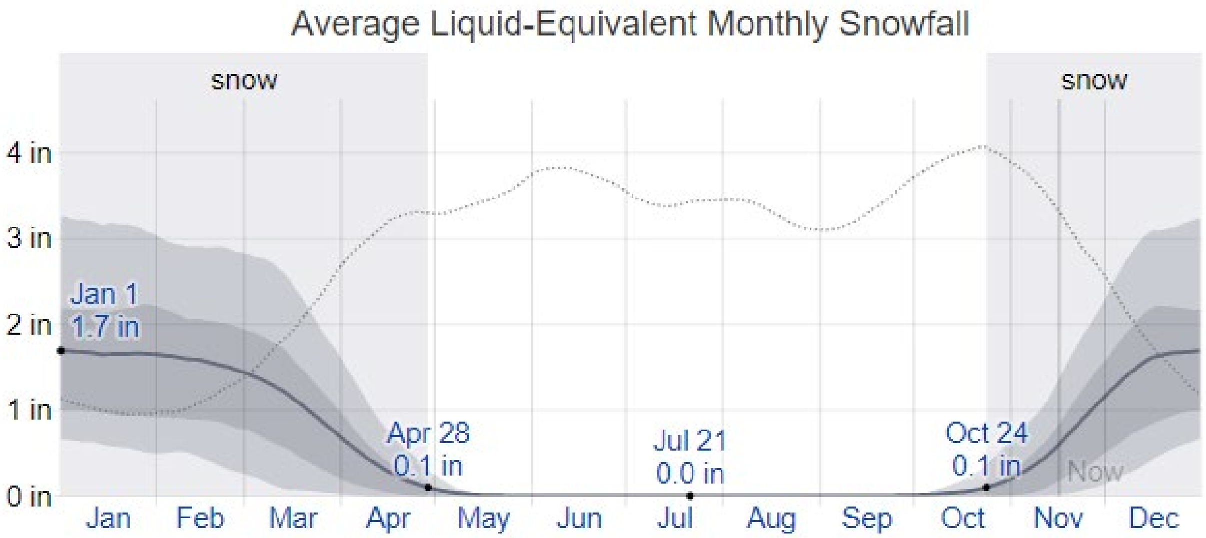

Figure 1.15. Seasonal precipitation in Fayette, Maine with the dotted line indicating average liquid rainfall and the solid line indicating average liquid-equivalent snowfall (https://weatherspark.com).

1.5. Previous Studies at Basin Pond

Several studies in the past utilize the varved sediment provided by Basin Pond to track various regional and global trends. Miller, (2015), tracked the effects of precipitation on varve thickness, showing that major storm events slightly match up with thicker varves (figure 1.16). Varve thickness likely does not perfectly match up with total precipitation because of biological processes and other events affecting sedimentation in the pond, meaning that sedimentation rates vary (Miller, 2015). Along with sedimentation data, Miller et al., (2017) studied forest fire activity and fossil fuel burning, which can indicate times of increased natural and anthropogenic lead deposition through the dissolution of the underlying bedrock, and impurities burned in fossil fuels. Using the polycyclic aromatic hydrocarbons (PAHs) retene and chrysene along with charcoal fragments within the lacustrine sediments, Miller et al., (2017) found an increase in fossil fuel burning from the 1850s to the 1900s with evidence for the existence of three specific regional wildfire events occurring in 1761-1762, 1825, and 1947 (figure 1.17). Miller et al., (2018) shows through the study of the algal lipids brGDGTs, that the paleotemperature profile varies with respect to others in the northeast United States, indicating potential times of decreased and increased global volcanic activity, releasing aerosols into the atmosphere (figure 1.18). These data may indicate that Basin Pond has a varying age model throughout time, with increased lead deposition in sediments from the 1850s to the 1900s and at times associated with increased forest fire and volcanic activity.

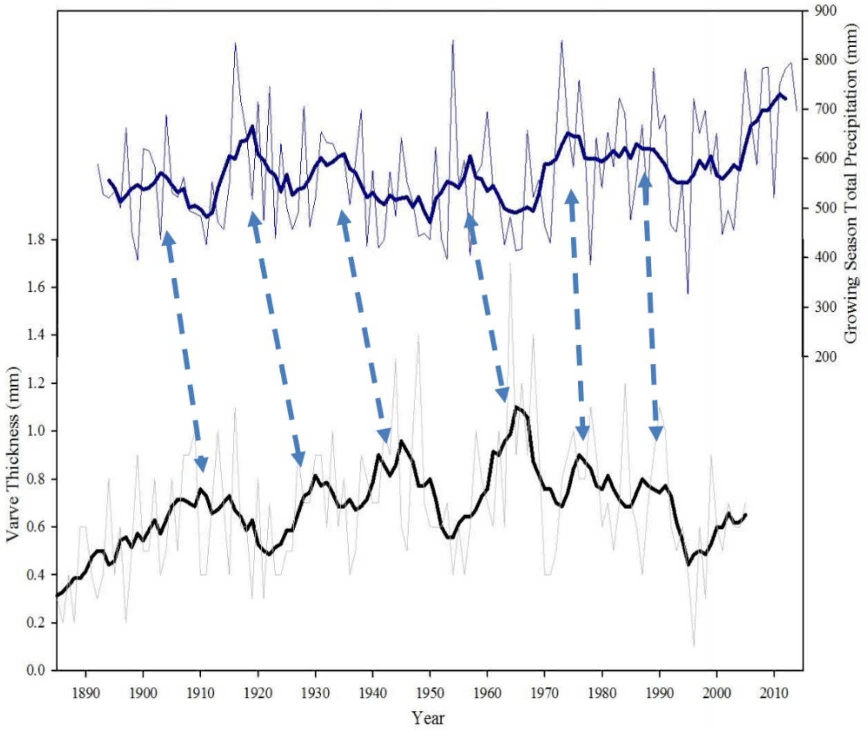

Figure 1.16. Correlation between varve thickness and weather patterns as interpreted by Miller (From Miller, 2015).

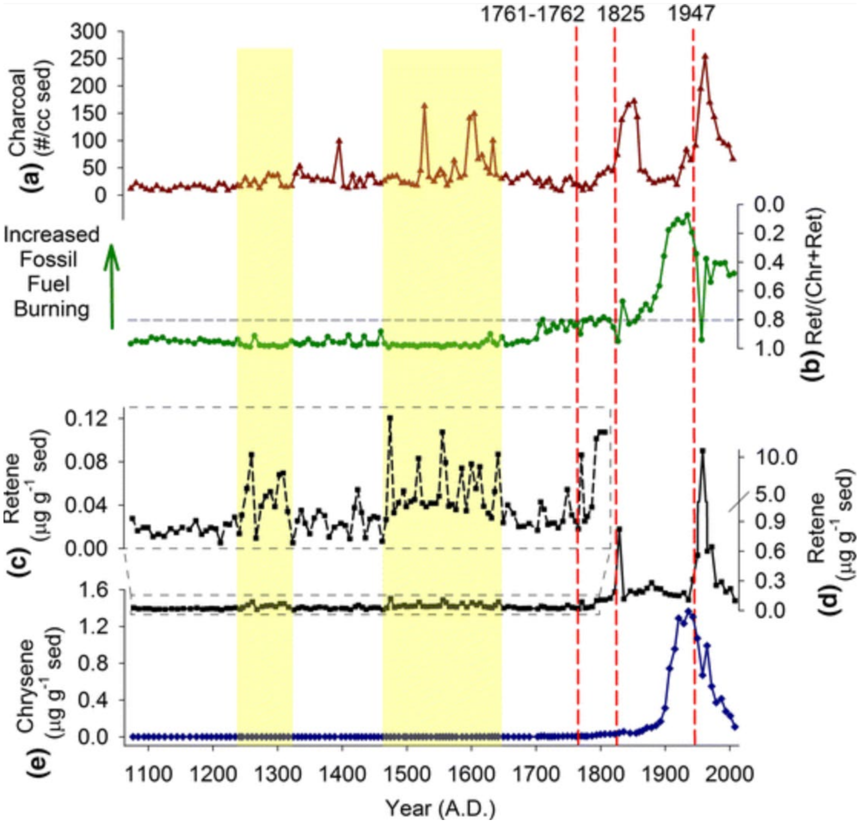

Figure 1.17. Graphs of retene, chrysene, charcoal presence, and fossil fuel burning lined up to show the correlation between them (From Miller et al., 2017).

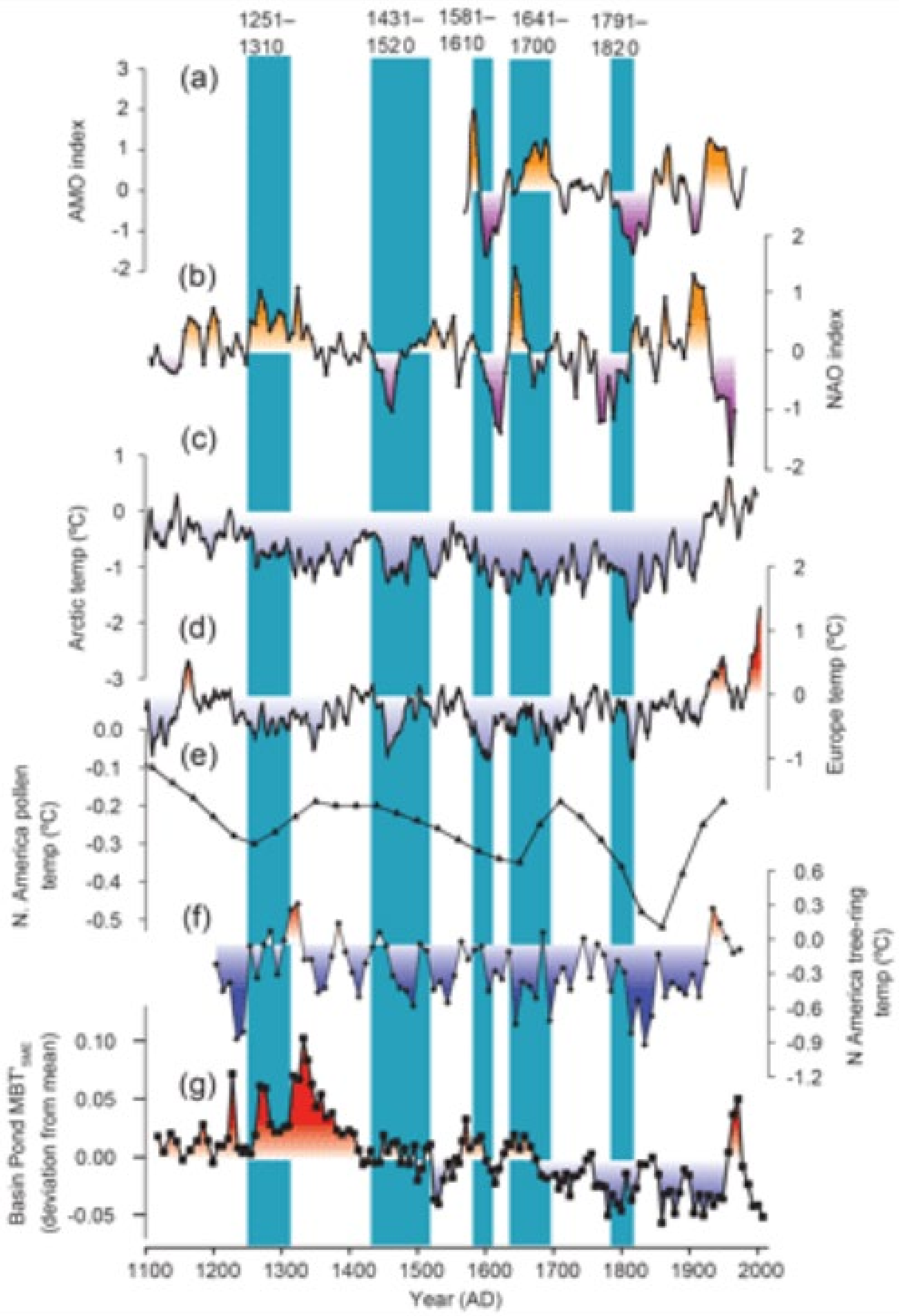

Figure 1.18. The variance in paleotemperature profiles with respect to Basin Pond indicating times of decreased volcanic activity highlighted in blue (From Miller et al., 2018).

Data collected in Acadia, Maine from Norton et al., (1995), currently provides the most detailed historical account of lead deposition in Maine with general lead accumulation rates in bioturbated sediment over the past century. The limited data gathered on lead 210 activity in Basin Pond showed the most change in activity happening between the years of 1938 to the present (Miller, 2015). Extensive work has been done on regional temperature and forest fire histories using Basin Pond sediments, but no record of industrialization as captured by lead concentration exists as of yet.

1.6. Intent of Project

Sedimentological and lead analyses both provide varying details on the overall health of Basin Pond and the environment around it, while also giving either data set temporal context. Analysis of lead content within Basin Pond shows atmospheric levels of lead over the centuries and therefore the impact humanity has on the environment. Sedimentological data places lead analysis in temporal context with the varved sequence, while also providing data on climate and major storms over the past 300 years. These data sets should both be valuable in finding how anthropogenic activity affects the state of the atmosphere, and in turn, lacustrine environments.

Chapter 2: Methods

2.1. Freeze Core collection

In May of 2018 on an overcast, rainy day, Professor Mike Retelle's spring short term class on Paleolimnology, of which I was a student, collected a freeze core from the deepest part of Basin Pond. A freeze corer is a hollow metallic wedge designed to be filled with a dry ice and methanol slurry at approximately -80 °C, and inserted into the sediment, freezing an outer layer of sediment to the device. To minimize disturbance of the sediment during collection, the corer is inserted quickly into the sediment layers before the layers freeze onto the core. This lack of disturbance results in the preservation of sedimentary structures in the core (figure 2.2).

The freeze coring device is approximately 0.75 meters long and 0.1 m wide. After filling the corer with dry ice and alcohol, we capped the top of the device and canoed the corer to the deepest point of Basin Pond to lower into the sediment (figure 2.1). Before core collection, we measured the depth of the deepest point in Basin Pond. To collect the core, we attached the device to a 35 meter rope, marking the exact point on the rope to lower the core to such that it was suspended just above the sediment water interface. At the rope marking, making sure to tightly hold the end of the rope, we dropped the corer into the sediment by releasing the rest of the rope. After waiting 10 to 15 minutes for the core to freeze onto the wedge, we slowly raised the corer into the canoe and paddled back to land.

Figure 2.1. Filling the hollow wedge with dry ice and isopropyl alcohol.

In the field, we used a cloth to wipe off the unfrozen mud on the outside of the core. We separated the core from the wedge by pouring out any remaining dry ice and alcohol, and adding hot water into the hollow wedge to allow the inside layer of the core to partially melt and slide off the wedge (figure 2.2). As the core was still frozen, separating it into separate slabs in the field would have been difficult. We filled the hollow tube of sediment with dried ice, wrapped it in aluminum foil, and stored it in a cooler filled with dried ice (figure 2.3).

We transported this core back to Bates College and placed it in a freezer to preserve its integrity.

Figure 2.2. Hollow core sample cleaned and taken off wedge.

Figure 2.3. Wrapping the frozen core in aluminum foil before putting it into cooler filled with dried ice.

2.2. Thin Section Creation

I created thin sections for the Basin Pond core to provide an age model for the core. I then intended to use this age model, paired with lead concentration data from the ICP-OES, to determine the time of lead deposition throughout the core.

I used a Dremel100XPR to cut the core into 4 separate slabs before storing them in a freezer. I created 15 open 2.5 x 7 x 1 cm aluminum boxes with holes drilled into them to hold the sediment samples during epoxy impregnation. I enscribed the bottom of each box with the author's initials, SO, the sample number, and the core collection date, spring of 2018, with arrows pointing to the top of the sample (figure 2.4).

Figure 2.4. Folded boxes next to an unfolded box, traced templates on the aluminum sheet, and the block used for drilling through the sheets.

I carefully measured and subsampled the core into 8 different 1 cm overlapping 1x7 cm segments, storing extra scraps in a bag for further analysis (figure 2.5). The 8 samples were then freeze dried in a Labconco Freezone 6 Freeze Dry system for 3 days.

Figure 2.5. First sample cut and placed in boat, with the top of the core and sediment-water interface to the left.

Using the proportions of 35.577% ERL, 12.370% DER, 51.185% NSA, and .8670% DMAE, I made 650 g of epoxy to impregnate the samples with. I carefully impregnated the samples in two separate plastic containers, used a vacuum chamber to remove air from the epoxy, and cured them in a Fisher Isotemp 500 Series oven at 60 °C for 5 days (figure 2.6).

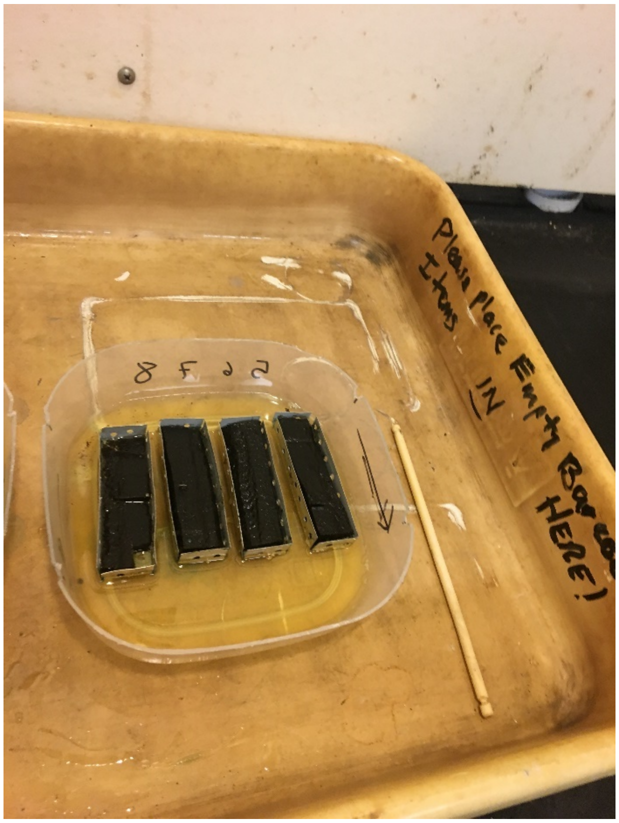

Figure 2.6. Epoxy impregnation of samples in the plastic containers.

I cut the samples apart using a Delta 10” bench saw and a Diamond Pacific 14” slab saw before sending them off to Quality Thin Sections in Tucson, Arizona to be created into thin sections (figure 2.7).

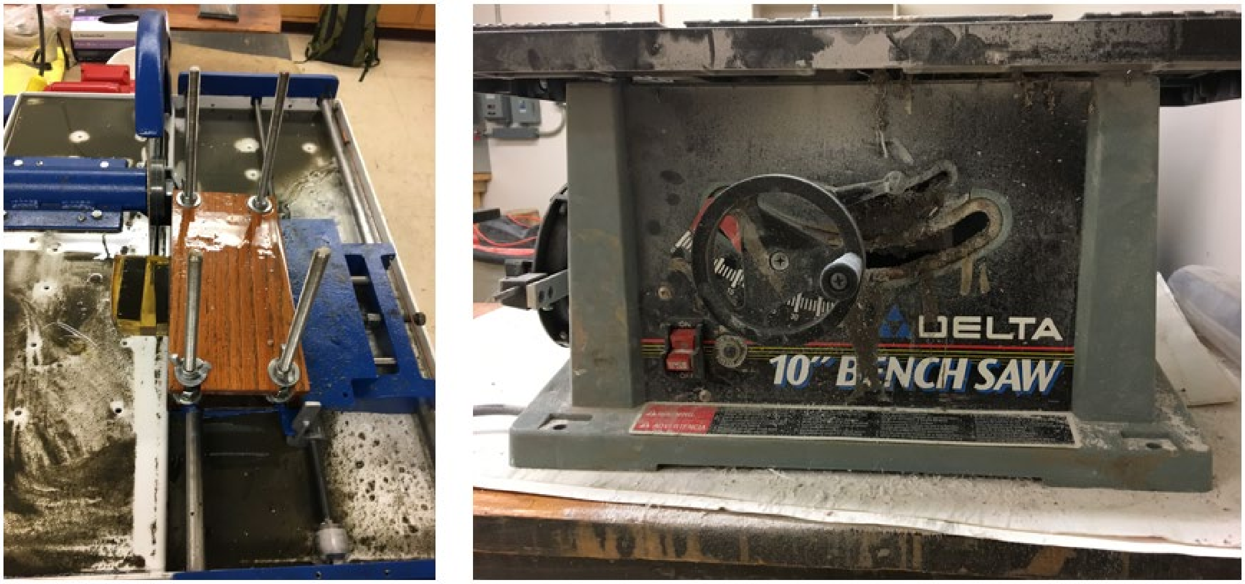

Figure 2.7. Bench saw (left) and Diamond Pacific saw (right) used to cut samples.

2.3. Sediment Lead Analysis

Samples were digested in concentrated nitric acid, and the resultant digestions were run on the ICP-OES. I conducted 3 separate runs of core samples on the ICP-OES. First, 7 homogenized sediment samples of varying weights and 2 blanks were run on 10/4/19 to test reproducibility of results and the least mass needed for a good lead signal. Once reproducibility of the results was established, I put two runs of freeze core samples through the ICP-OES on 10/15/19 and 10/25/19 in batches of 24, each with a procedural blank. These tests all followed similar procedures.

2.3.1. Preparation for ICP-OES Analysis

I scored and cut the slabs in 1cm increments downcore using a Dremel 100XPR and stored the resultant samples in a freezer. I used the Labconco Freezone 6 Freeze Dry System to freeze dry the samples, for approximately 3 days and stored them at room temperature before preparation for ICP-OES analysis.

A CEM MARS 5 Xtraction 230/60 microwave was used to digest dry sediment samples ~.5g in weight in 10.0 mL concentrated nitric acid for several hours at 175 °C. Before usage, I cleaned the vessels with hydrochloric acid and ran them through the microwave with just nitric acid. I diluted each resultant sample digest and stored the samples in separate 15 ml centrifuge tubes.

I used the SPEX CertiPrep ICP-OES standard solution 2 with calibrated Mohr pipettes and micropipettes to make 50 ml volumes of .01, .1, 1, and 10 ppm concentrations of the standard (table 1). Additionally I made 1L of a 2% nitric acid solution by diluting the 18 molar nitric acid with e-pure water using acid-washed glassware.

Table 1. Volumes of standard or diluted solutions needed to make each concentration of standard with dilution up to 50 ml.

Concentration of standard solution (ppm)	Volume needed (ml)
10	5ml standard
1	.5ml standard
.1	5ml of 1ppm
.01	.5ml of 1ppm

2.3.2. ICP-OES Analysis

The ICP-OES finds the concentration of ions in a given solution by separating the ions from the solution, exciting them to a plasma, and measuring the intensity of various wavelengths given off through the transition of the ions back to their initial state (Harris, 1999). I used an iCAP 6000 series ICP-OES to measure the lead concentrations for the standard solutions, 24 digested thick sediment samples, and 24 digested thin sediment samples. I used the program ICS2 10ppm high standard to run the samples, with 2% nitric acid as a cleaning agent for the sampler.

The ICP-OES collected counts per second data for each ion in solution, which it translated to parts per million for each ion. I looked at each set of averages for each ion to find out which data was usable and which data contained too much background noise. Using the data collected on lead, I was able to use the parts per million number given to calculate $\frac{mg\ Pb}{kg\ sed}$.

Chapter 3: Results

3.1. Physical Description of Core

As seen in figure 2.2 in the methods, the varved core changes from having groups of lighter and darker sediments at the top section of the core to having a more homogenous color near the bottom of the core with constant variation in dark/light layers every year. The core was approximately 49 cm long, 10 cm wide for the wider slab, and 4.5 cm wide for the thinner slab. The thin sections created from the thin side of the core show that the varves are slightly deformed and difficult to count in areas (figure 3.1), so it is impossible to effectively estimate the exact date of sedimentation at any particular point in the core using the thin sections.

Figure 3.1. Thin section from the top of the core, showing mixing of the sediment throughout the section with the sediment-water interface in the top of the section.

3.2. ICP-OES Running Conditions

3.2.1. Calibration Curves

Three different calibration curves were generated, one on each day the ICP-OES and samples were run. The two curves for the runs completed on 10/15/19 and 10/4/19 were nearly identical, but the curve for the run on 10/25/19 was drastically different. The instrument was cleaned between the run completed on 10/15/19 and 10/25/19, so the sensitivity of the instrument increased significantly, changing the slope of the curve from 80.6 to 829.6 (figure 3.2). The R^2 values for all 3 runs were all close to or exactly 1, meaning the ICP-OES was calibrated for every run.

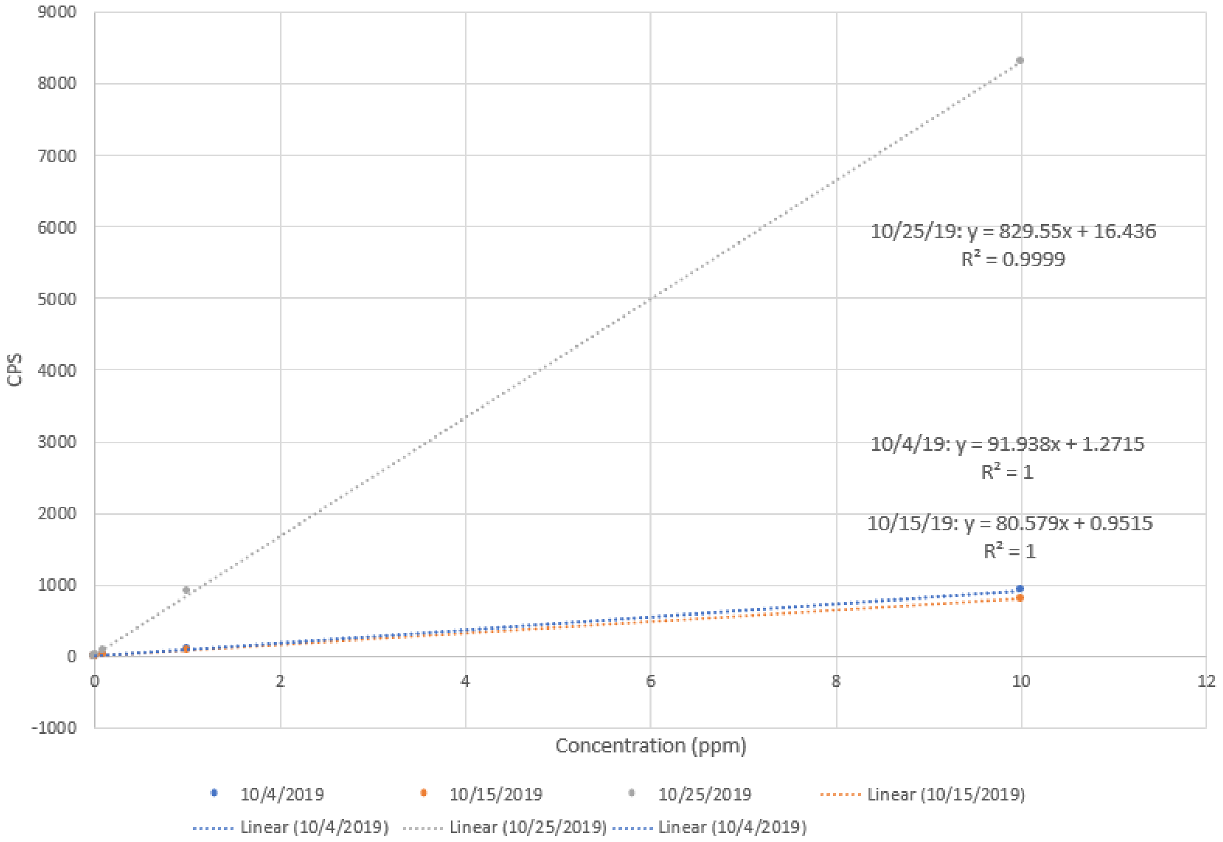

Figure 3.2. Calibration curves (CPS vs. concentration in ppm) for the three different runs on 10/4/19, 10/15/19, and 10/25/19. Note the variation in slopes between runs on 10/15/19 and 10/25/19.

3.2.2. Interference Data

In graphing CPS versus wavelength, the sediment sample showed background levels of approximately 300 CPS, silmilar to that of the 1ppm sample standard (figure 3.3). This comparison validates the fact that the machine is reporting accurate concentration values.

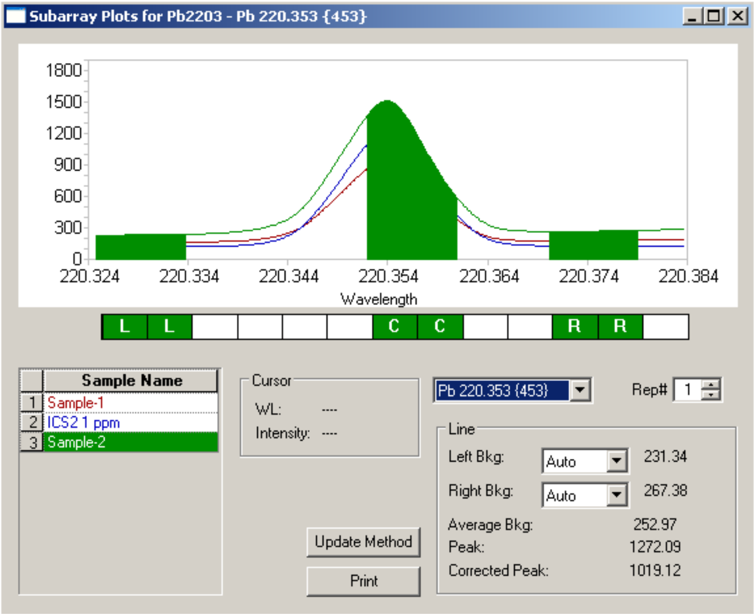

Subarray Plots for Pb2203 - Pb 220.353 {453}

	Sample Name
1	Sample-1
2	ICS2 1 ppm
3	Sample-2

WL: ----
Intensity: ----

Pb 220.353 {453}
Rep# 1

Left Bkg: Auto 231.34
Right Bkg: Auto 267.38
Average Bkg: 252.97
Peak: 1272.09
Corrected Peak: 1019.12

Figure 3.3. Checking interference of the Pb 220.3 line in a sample in comparison to the 1ppm standard solution. Note the constant background levels at around 300 CPS.

3.3. Homogenized Core Sediment ICP-OES Data

Concentration tests of varying weights of homogenized sediment tested the reproducibility of the results and determined the lowest mass of sediment needed for a reliable lead signal. Lead concentrations of heavier samples from .00025-.0005 kg are closer to the mean lead concentration of 13.61 mg Pb/kg sediment than lighter samples from .00005-.0002214 kg, meaning that samples above .00025 kg give the best lead signal (figure 3.4 and table 3.1). The mean deviation from the average for the homogenized samples above .00025 kg is 1.007 mg Pb/kg sed; this value is used to make the error bars for the core samples.

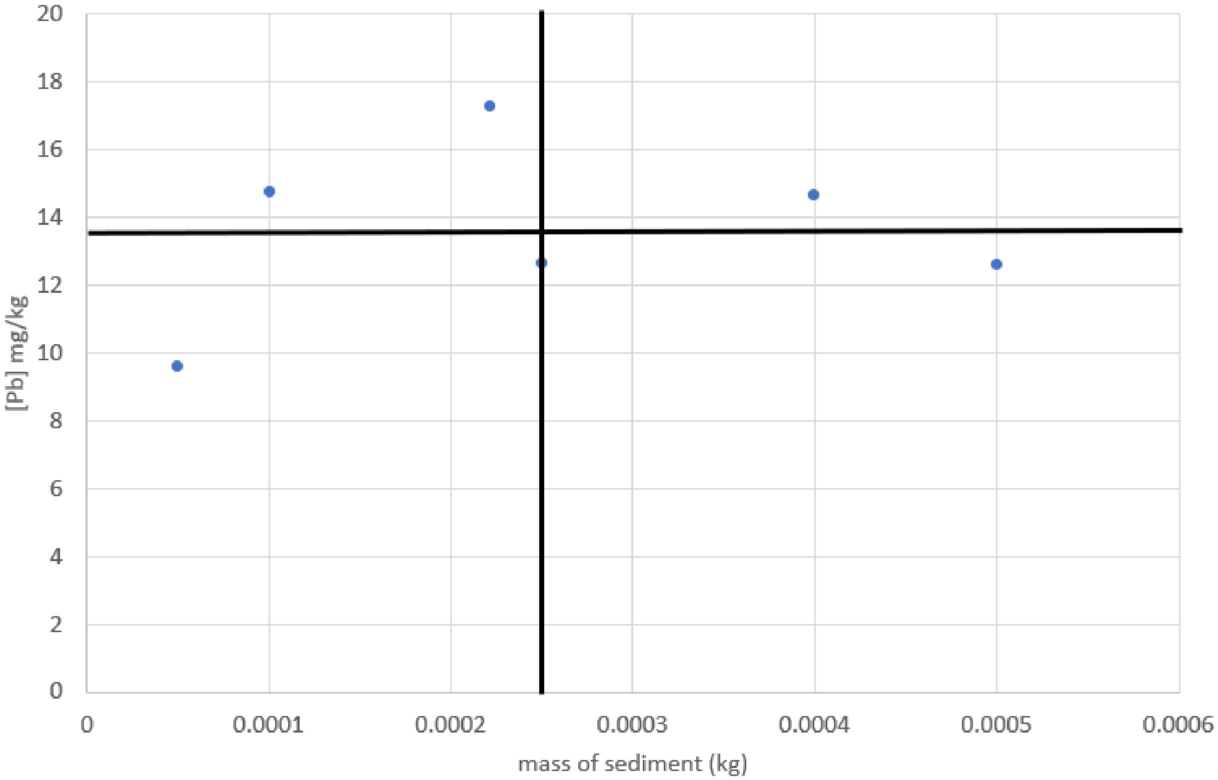

Figure 3.4. Homogenized sediment samples, with the average measured concentration represented by the horizontal black line and lower variation in lead concentration for sediment masses greater than .00025 kg, shown to the right of the vertical line.

Table 3.1. Homogenized core sediment weights, concentrations, average concentration, and deviations from average. Note the lower deviation from the average for heavier samples.

Core sediment weight (kg)	Concentration (mg Pb/kg sed.)	Average concentration (mg Pb/kg sed.)	Deviation from Average (mg Pb/kg sed.)
.0005000	12.62	13.61	.9898
.0003996	14.69	-	1.080
.0002500	12.66	-	.9498
.0002214	17.32	-	3.710
.0001000	14.75	-	1.140
.00004990	9.619	-	3.991

3.4. ICP-OES Data

Lead line 220.3 nm concentraiton data along the core for combined and single sediment samples are plotted with respect to depth (figure 3.5). The table in appendix A displays the plotted data numerically. Lead concentrations range from 3.42 – 119.38 mg lead/kg of sediment (ppm) throughout the core. Background lead concentrations, as defined by values in the lower part of the core, between 41 to 45 cm, generally stay constant at around 5 ppm. The concentration rises from 28 cm to 25 cm by 10.4 ppm and then decreases by 9.4 ppm from 25 cm to 20 cm. A second rise in concentration of 109.22 ppm occurs between 10 cm and 3 cm, with a slight fall of 10.04 ppm between 3 cm and 2 cm following it. A final rise in lead concentration happens between 2 cm and 0 cm of 26.54 ppm.

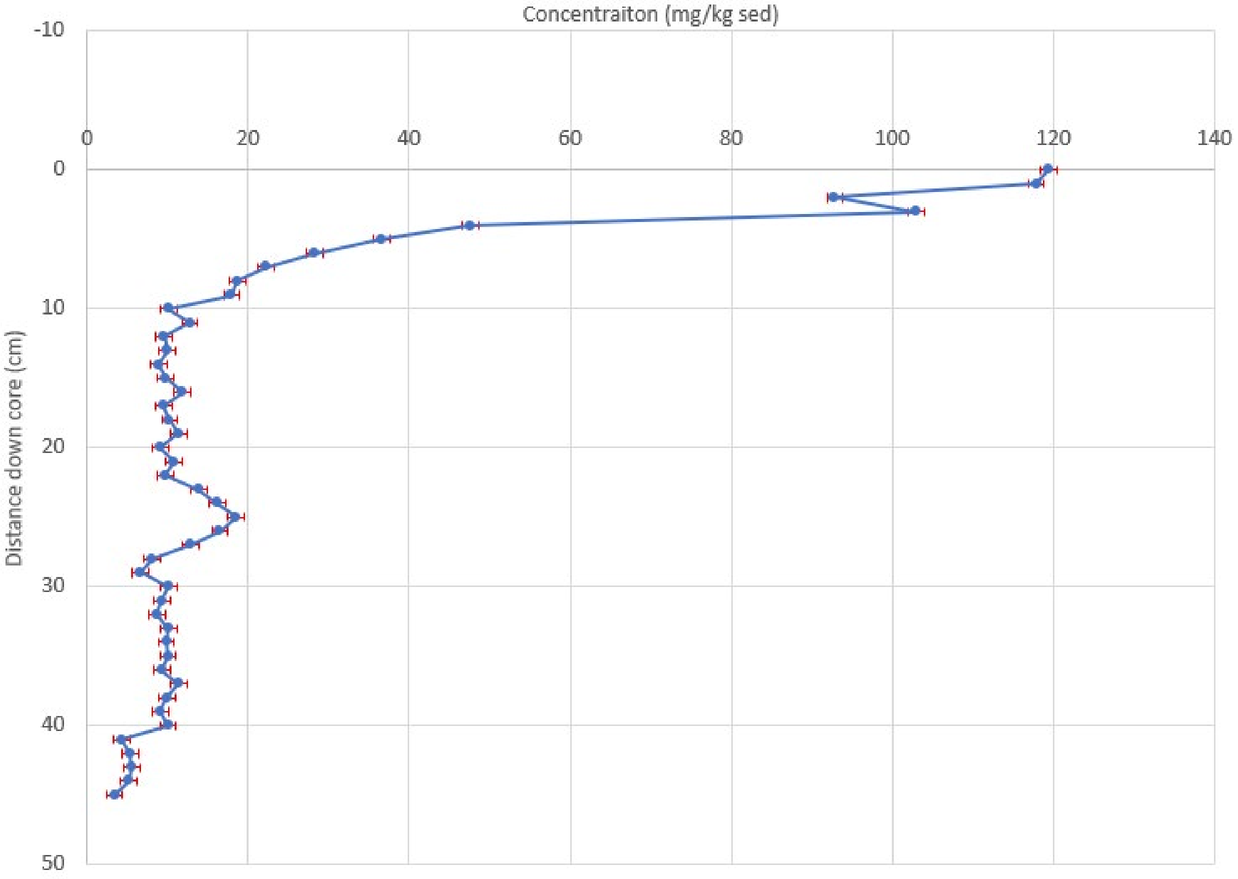

Figure 3.5. Lead concentration in mg Pb/kg sediment versus depth down core. Error bars are in red, calculated from the homogenized sediment deviation from the average. Blue data points show the first run of samples through the ICP, orange data points show the second run of samples, and grey data points show the samples which combined 2 sides of the core in the second run.

3.5. Sources of Error

Though the data appear well-correlated and calibrated, several sources of error may affect the accuracy of the results. A few main sources of error likely contribute most significantly to errors in the data set. The entirety of the core could not be run all at once, so two separate runs of the core data allowed for more room for error. The act of using a straight edge to score and cut the uneven icy core was difficult and required estimation of where to cut even with an accurate ruler. The dremel blade removed anywhere from 1-3 mm of sediment out of the core while cutting the slabs, and the removal of sediment causes inaccuracies in the true age range of each sample. Smaller sources of error could be attributed to the core collection or labwork.

Gravitational compression of sediments near the bottom of the core could result in a deviation from a constant age model, and the corer may not have been perfectly vertical in the sediment during core collection. In the lab, during weighing of the sediment, slight breezes and static electricity disturbed and dispersed the sediment, and vibrations as well as static eletricity affected the accuracy of the scale. Cross contamination of samples is also always possible during dilutions of the samples with e-pure water, though experimental blanks produced negative lead concentrations, indicating low levels of contamination.

The thin sections were likely muddled because they were created from one of the thin slabs of the core and freeze dried before epoxy impregnation, allowing for more potential for varve disruption.

Chapter 4: Discussion

4.1. Age Model Variation

Several age models exist describing Basin Pond sedimentation. Miller, (2015), used age models between 14.08-17.54 years/cm calculated from varve counts, radioisotopic dating from lead 210, and radiocaron dating for his studies on the history of Basin Pond before 1950. Dan Frost, (2005), used an age model of 6.6 years/cm for the upper sediment in Basin Pond. The averaged age model value of 15.31 years/cm calculated from the Miller, (2015) study is a better fit for the lead concentration data because it averages out the error associated with all three of the models, providing the most accurate average varve thickness for the sediment. Assuming an age model of 15.31 years/cm, the core is approximately 689 years old (figure 4.1).

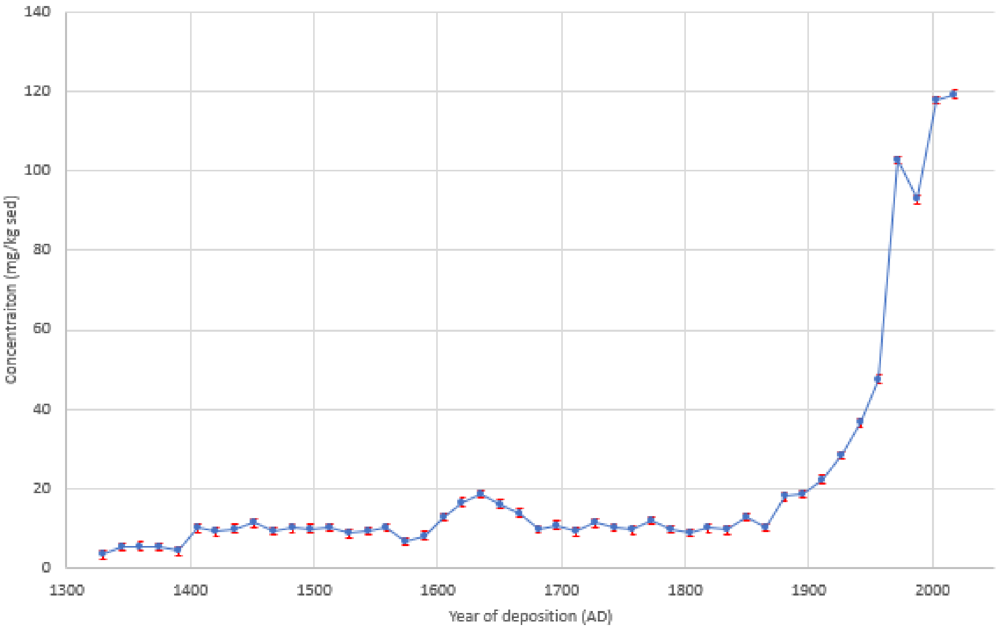

Figure 4.1. Basin Pond lead concentration versus year of deposition assuming an age model of 15.31 years/cm, calculated from Miller, (2015), with the deviation from each measurement in red.

The Basin Pond core exhibits 5 separate changes in lead concentrations: a rise from 1390 – 1405, a rise and fall between 1589 – 1681 with a peak at 1619, a rise from 1864-1880, a rise and fall between 1895 – 1987 with a peak at 1972, and a final rise from 1972 – 2018. These 5 separate changes in lead concentration can be explained through lead emissions throughout the state, country, and world.

4.2. Trends in Lead Concentration

4.2.1. Trends from 1390 – 1880

There is a sudden rise in lead concentration from the late 1300s to the early 1400s. According to Miller et al., (2017), a regional forest fire event occurred in the early 1400s, which may have triggered increased erosion of the underlying rock and transportation of plant matter containing lead into Basin Pond, increasing the resultant lead concentration.

A rise and fall in lead concentration exists from 1574 – 1666 with a maximum at 1619. In Virginia, (figure 4.2) there was increased mining in the late 1500s and the early 1600s, with a decline at around 1612 due to the rise of tobacco plantations, so that could have resulted in the increase in atmospheric lead emissions (Heuvel, 2007). There was also increased forest fire activity around Basin Pond between the 1500s and early 1600s, which may have contributed to part of the rise seen during this time (Miller, 2017).

The sudden rise in lead concentration from 1879 – 1882 can be attributed to metal mining in Maine. Much of the mining in Maine consisted of mining non-metallic materials until 1848 with the mining of iron ore at Katahdin Iron Works and the creation of the charcoal furnace nearby (Lepage et al., 1990). Maine went through a metal mining boom from 1879 to 1882 with the creation of mines at Blue Hill, Sullivan, Acton, and Lubec due to men returning from the goldrush (Lepage et al., 1990). The mine at Acton is upwind of Basin Pond, so activity from that mine likely contributed to the sudden increase in atmospheric lead concentration seen from 1864 – 1880 (figure 4.2). Maine exhibited a decrease in mining activity after the end of the metal mining boom, which explains the slight plateau seen after the initial sudden increase (Lepage et al., 1990).

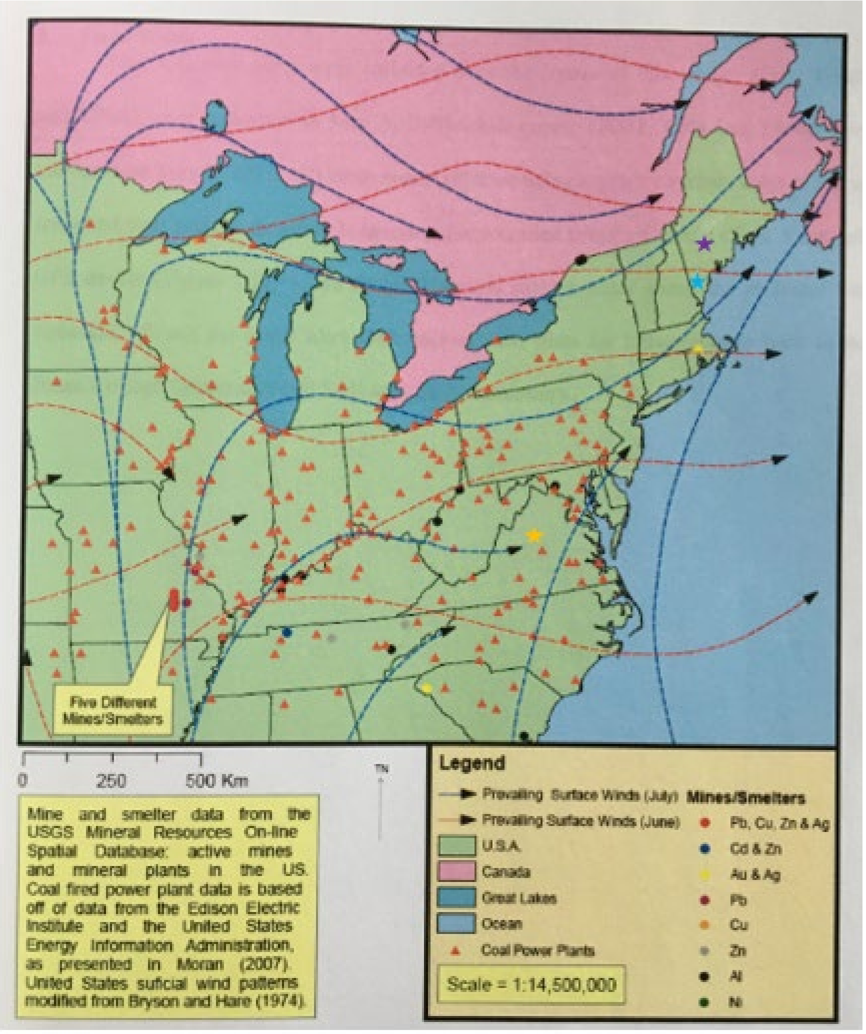

Mine and smelter data from the USGS Mineral Resources On-line Spatial Database: active mines and mineral plants in the US. Coal fired power plant data is based off of data from the Edison Electric Institute and the United States Energy Information Administration, as presented in Moran (2007). United States suficial wind patterns modified from Bryson and Hare (1974).

Figure 4.2. Wind currents throughout the eastern United States (Modified from Eberle, 2008). The purple star indicates the location of Basin Pond, the orange star shows the location of Virginia, and the blue star is the location of Acton Maine.

4.2.2. Trends from 1895 – 1987

The initial rise in lead concentration from 1900 – 1920 can be attributed to coal burning and ore smelting in the industrial revolution (Graney et al., 1995). Studies throughout the US provide significant evidence for increased usage of leaded gasoline from the 1920s to the 1970s, followed by the fall in leaded gasoline due to the effects of the Clean Air Act in the 1970s (Holland and Turekian, 2004; Graney et al., 1995; Siver and Wozniak, 2001; Norton et al., 1995; Callender and Metre, 1997). The rise and fall in lead concentration seen in Basin Pond from 1895 – 1987 can therefore be attributed to this cause.

4.2.3. Rise from 1987 – 2018

Annual lead production from mining has decreased significantly from the 1980s to the present in Canada and the United States (Mudd, 2009). Many of the cores from the United States exhibit a decrease in lead concentrations from the 1970s to the present, so the increase in lead concentration in the Basin Pond core after the decrease in the 1970s is somewhat of an anomaly (Holland and Turekian, 2004). World production of lead from mining over the past hundred years show an increase in lead production from the 1990s to the present (figure 4.3; Mudd, 2009). This increase generally comes from Chinese production of lead (Mudd, 2009). The increase in carbon dioxide emissions due to the combustion of fossil fuels exhibits a similar trend over the past 20 years, with a spike in Chinese fossil fuel emissions (figure 4.4; Quere et al., 2016). Wind currents show that pollutant pathways through the atmosphere can feasibly travel from China, to the Western United States, and eventually to Maine (Marx and McGowan, 2010). It may be possible that lead concentrations in Basin Pond increase from 1987 to the present due to increased lead mining and fossil fuel emissions in China and other countries (Mudd, 2009).

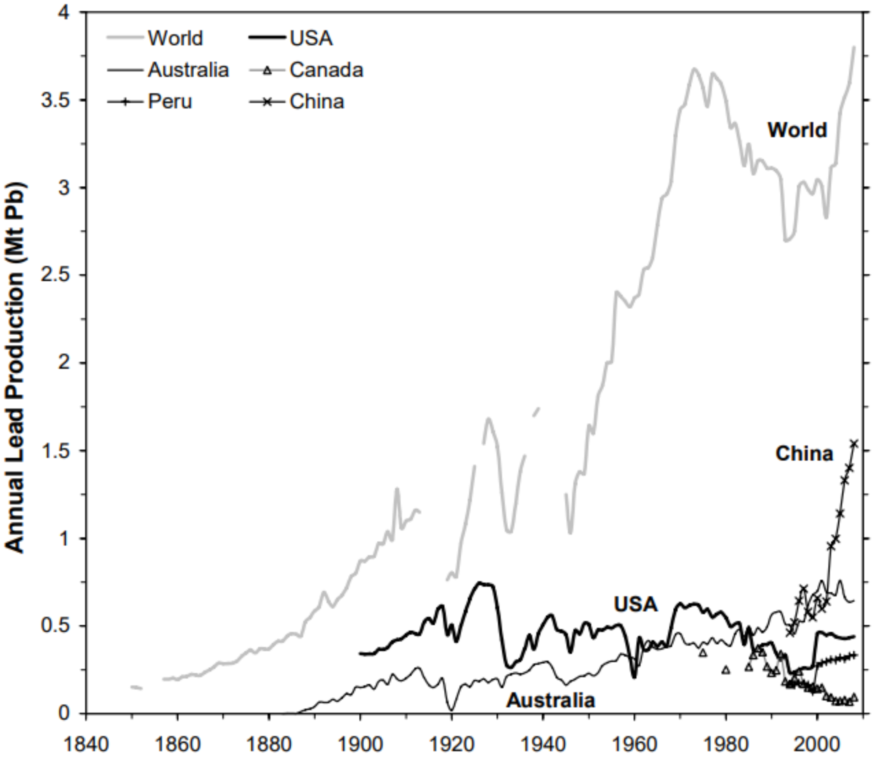

Figure 4.3. Production of lead over the past century for several countries in the world (From Mudd, 2009).

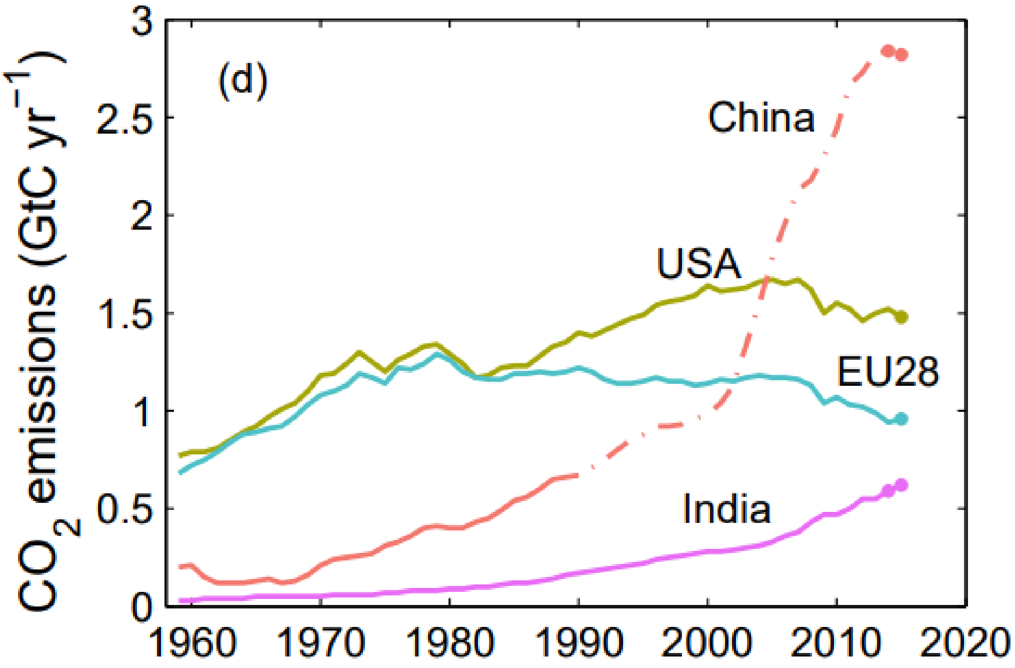

Figure 4.4. World production of carbon dioxide due to the burning of fossil fuels (From Quere et al., 2016).

4.3. Context and Implications for Atmospheric Lead Concentration

Increased lead concentrations in the atmosphere can significantly impact human life. In the 1970s, people, on average, had blood lead levels of approximately 12.8 µg/dl, which differs significantly from the blood levels seen in 2000, at 2.8 µg/dl (Tong et al., 2000). This decrease in blood lead levels is reassuring, showing the effects of the decrease in usage of leaded gasoline (Tong et al., 2000). However, Basin Pond sediments indicate an increase in atmospheric lead concentrations in Fayette, Maine up to ~120 ppm, which is similar to lead concentration levels in mid-American lake sediments in the 1970s (Callender and Metre, 1997). This contradictory rise in lead concentration reveals that atmospheric lead concentration may generally be higher than previously thought, increasing the likelihood of chronic exposure to lead (Tong et al., 2000). This newfound information begs the question of whether lead levels will increase or stabilize in the future and what effects this will have on the communities living in Maine, the United States, and the world.

Chapter 5: Conclusions

Anthropogenic activity significantly impacts atmospheric lead concentrations. Three major trends in atmospheric lead concentration exist in the sediment record: the rise and fall from 1590 – 1681, the rise and fall from 1895 – 1987, and the rise from the 1990s to the present. The effects of Virginians switching from mining to tobacco farming in the early 1600s can explain the 1590 – 1681 rise and fall in lead concentration. The rise in the usage of leaded gasoline and fall due to the Clean Air Act in automobiles in the 1900s can describe the trends seen from 1895 – 1987. The rise from the 1990s to the present can be attributed to increased lead mining and fossil fuel burning in China, as well as a few other industrialized countries. According to Basin Pond sediments, atmospheric lead levels are rising, and although steps like the Clean Air Act have been taken to decrease lead concentration in the environment, more action needs to be taken to end lead emissions altogether.

Chapter 6: Future Studies

The upwards trend in lead concentration seen from the 1980s to the present in Basin Pond is worrisome, and should be investigated further in other New England ponds with undisturbed sediment to see if there are any similarities in lead concentration trends. If similar trends exist in recent years, then the collection of isotopic data could identify sources of lead emissions, aiding in the efforts to end environmental emissions. Presently at Basin Pond, through several studies, there exist several age models which describe its varved sediment, but no two are alike, meaning that work still needs to be done which provides a consistent age model for the sediment at various localities throughout the lake.

References Cited

Borns Jr., H.W., Doner, L.A., Dorion, C.C., Jacobson Jr., G.L., Kaplan, M.R., Kreutz, K.J., Lowell, T.V., Thompson, W.B., and Weddle, T.K., 2004, The Deglaciation of Maine, USA: The University of Maine Earth Science Faculty Scholarship, 276, p. 1-20.

Bradley, D.C., Tucker, R.D., Lux, D.R., Harris, A.G., and McGregor, D.C., 1999, Migration of the Acadian Orogen and Foreland Basin Across the Northern Appalachians of Maine and Adjacent Areas: U.S. Geological Survey, Professional Paper 1624, p. 1-49.

Callender, E., and Metre, P.C.V., 1997, Reservoir Sediment Cores Show U.S. Lead Declines: Environmental Science & Technology, v. 31, p. 424-428.

Eberle, D.E.H., 2008, Three Hundred Years of Lead Deposition in Taylor Pond, Auburn, Maine [Undergraduate Thesis]: Bates College, 77 p.

Frost, D.S., 2005. Paleoclimate Reconstruction using Physical Sedimentology and Organic Matter Biogeochemistry of Varved Sediments, Basin Pond, Fayette, ME [Undergraduate Thesis]: Bates College, 162 p.

Graney, J.R., Halliday, A.N., Keeler, G.J., Nriagu, J.O., Robbins, J.A., and Norton, S.A., 1995, Isotopic record of lead pollution in lake sediments from the northeastern United States: Geochimica et Cosmochimica Acta, v. 59, p. 1715-1728.

Guidotti, C.V., 1989, Metamorphism in Maine: An Overview: Studies in Maine Geology, v. 3, p. 1-17.

Harris, D.C., 1999, Atomic Spectroscopy, in Julet M.R., Quantitative Chemical Analysis (fifth edition): W.H. Freeman and Company New York, p. 615 – 639.

Holland, H.D., and Turekian, K.K., ed., 2004, Treatise on Geochemistry, *in* Lollar, B.S., ed., Environmental Geochemistry, volume 9: Oxford, UK, Elsevier, p. 67-105.

Heuvel, L.L., 2007, Early Attempts of English Mineral Exploration in North America: The Jamestown Colony: Virginia Division of Mineral Resources Publication 176, 40 p.

Lepage, C.A., Foley, M.E., and Thompson W.B., 1990, Mining in Maine: Past, Present, and Future: Maine Geological Survey, 14 p.

Marx, S.K., and McGowan, H.A., 2010, Long Distance Transport of Urban and Industrial Metals and Their Incorporation into the Environment: Sources, Transport Pathways and Historical Trends, *in* Zereini, F., and Wiseman, C.L.S., eds., Urban Airborne Particulate Matter, p. 103-124.

Matthieu, S.A., 1909, The History of Dutchess County New York: New York, Higginson Book Company, p. 791.

Miller, D.R., 2015, A High Resolution Paleoenvironmental and Paleoclimatic History of Extreme Events on the Laminated Sediment Record from Basin Pond, Fayette, Maine, U.S.A. [Masters Thesis]: University of Massachusetts Amherst, 133 p.

Miller, D.R., Castaneda, I.S., Bradley, R.S., and MacDonald, D., 2017, Local and regional wildfire activity in central Maine (USA) during the past 900 years: Journal of Paleolimnology, v. 58, p. 455-466, doi: 10.1007/s10933-017-0002-z.

Miller, D.R., Habicht, M.H., Keisling, B.A., Castaneda, I.S., and Bradley, R.S., 2018, A 900-year New England temperature reconstruction from in situ seasonally produced branched glycerol dialkyl glycerol tetraethers (brGDGTs): Climate of the Past, v. 14, p. 1653-1667, doi: https://doi.org/10.5194/cp-14-1653-2018.

Mudd, G.M., 2009, Historical Trends in Base Metal Mining: Backcasting to Understand the

Sustainability of Mining: Proceedings of the 48th Annual Conference of Metallurgists: Sudbury, Ontario, Canada, p 1-10.

Murphy, J.B., Keppie, J.D., Nance, R.D., Dostal, J., 2007, The Acadian Orogeny in the Appalachian Orogen: International Geology Review, v. 47, p. 668-687.

Norton, S.A., Evans, G.C., and Kahl, J.S., 1997, Comparison of Hg and Pb Fluxes to Hummocks and Hollows of Ombrotrophic Big Heath Bog and to Nearby Sargent Mt. Pond, Maine, USA: Department of Geological Sciences, University of Maine

Norton, S.A., Jacobson, G.L., Kopacek, J., and Navratil, T., 2016, A comparative study of long-term Hg and Pb sediment archives: Environmental Chemistry, v. 13, p. 517-527, doi: 10.1071/EN15114.

Osberg, P.H., Hussey, A.M., and Boone, G.M., 1985, Bedrock Geologic Map of Maine: Maine Geological Survey, scale 1:500,000.

Quere, C.L., et al., 2016, Global Carbon Budget 2016: Earth System Science Data, v. 8, p. 605 – 649.

Schubring, S.L.S., 1933, A Statistical Study of Lead and Zinc Mining in Wisconsin: Wisconsin Academy of Sciences, Arts, and Letters, v. 22, p. 1-98.

Settle, D.M., and Patterson, C.C., 1982, Magnitudes and Sources of Precipitation and Dry Deposition Fluxes of Industrial and Natural Leads to the North Pacific at Enewetak: Journal of Geophysical Research, v. 87, p. 8857-8869.

Siver, P.A., and Wozniak, J.A., 2001, Lead analysis of sediment cores from seven Connecticut lakes, Journal of Paleolimnology: v. 26, p. 1-10, doi: https://doi.org/10.1023/A:1011131201092.

Thompson, W.B., and Smith, G.W., 2008, Surficial geology of the Fayette quadrangle, Maine: Maine Geological Survey, Open-File Map 08-44, map, scale 1:24,000.

Tiwari, S., Tripathi, I.P., Tiwari, H.L., 2013, Effects of Lead on Environment: International Journal of Emerging Research in Management & Technology, v. 2, p. 1-5.

Tong, S., Schirnding, Y.E.V., and Prapamontol, T., 2000, Environmental lead exposure: a public health problem of global dimensions: Bulletin of the World Health Organization. v. 78, p. 1068-1077.

U.S. Geological Survey, 1996, Basin Pond Fayette, Kennebec County, Livermore, Maine (7.5): https://www.maine.gov/ifw/docs/lake-survey-maps/kennebec/basin_pond.pdf (accessed September 2019).

Zolitschka, B., 2007, Varved Lake Sediments, *in*: Elias, S.A., ed., Encyclopedia of Quaternary Science: Elsevier Science, p. 3105-3114.

Zolitschka, B., and Enters, D., 2009, Lacustrine Sediments, *in*: Gornitz, V., ed., Encyclopedia of Paleoclimatology and Ancient Environments: Springer, Dordrecht, p. 485-524.

Appendix A: ICP-OES data

ICP-OES Run date	Distance down core (cm)	ICP concentration (mg/L)	Mass of sample (g)	Concentration (mg Pb/kg sediment)
10/15/19	(blank)	-0.0046	0	-0.0046
10/25/19	(blank)	-0.0225	0	-0.0225
10/25/19	0-1	0.7908	0.1656	119.4
10/25/19	1-2	1.235	0.262	117.8
10/25/19	2-3	0.8443	0.2273	92.86
10/25/19	3-4	0.6957	0.169	102.9
10/25/19	4-5	0.497	0.2611	47.59
10/25/19	5-6	0.5797	0.3957	36.62
10/25/19	6-7	0.4686	0.4145	28.26
10/25/19	7-8	0.5633	0.6323	22.27
10/25/19	8-9	0.4547	0.6085	18.68
10/25/19	9-10	0.5025	0.7002	17.94
10/25/19	10-11	0.1245	0.3062	10.16
10/25/19	11-12	0.2098	0.4108	12.77
10/25/19	12-13	0.1596	0.4167	9.580
10/25/19	13-14	0.17	0.4255	9.990
10/25/19	14-15	0.1499	0.4216	8.890
10/25/19	15-16	0.1816	0.4641	9.780
10/25/19	16-17	0.2544	0.5348	11.89
10/25/19	17-18	0.1581	0.4141	9.540
10/25/19	18-19	0.0993	0.4837	10.26
10/25/19	19-20	0.1155	0.5061	11.41
10/25/19	20-21	0.0967	0.531	9.110
10/25/19	21-22	0.0922	0.426	10.82
10/15/19	22-23	0.0947	0.4872	9.720
10/15/19	23-24	0.1336	0.4825	13.84
10/15/19	24-25	0.1541	0.4768	16.16
10/15/19	25-26	0.1633	0.4411	18.51
10/15/19	26-27	0.129	0.391	16.50
10/15/19	27-28	0.1003	0.3904	12.85
10/15/19	28-29	0.0528	0.3254	8.110
10/15/19	29-30	0.0383	0.2868	6.680
10/15/19	30-31	0.05	0.2464	10.15
10/15/19	31-32	0.052	0.2805	9.270
10/15/19	32-33	0.0557	0.3203	8.690
10/15/19	33-34	0.0685	0.3379	10.14
10/15/19	34-35	0.0872	0.4413	9.880
10/15/19	35-36	0.1071	0.5314	10.08
10/15/19	36-37	0.1072	0.5755	9.310
10/15/19	37-38	0.1517	0.6667	11.38

10/15/19	38-39	0.1185	0.5968	9.930
10/15/19	39-40	0.1106	0.6088	9.080
10/15/19	40-41	0.1015	0.504	10.07
10/25/19	41-42	0.0604	0.3517	4.290
10/25/19	42-43	0.0729	0.3402	5.360
10/25/19	43-44	0.0665	0.3011	5.520
10/25/19	44-45	0.0609	0.2924	5.210
10/25/19	45-46	0.0248	0.1814	3.420